

# Integration of transient strain events with models of plate coupling and areas of great earthquakes in southwest Japan

Zhen Liu,<sup>1</sup> Susan Owen,<sup>1</sup> Danan Dong,<sup>1</sup> Paul Lundgren,<sup>1</sup> Frank Webb,<sup>1</sup> Eric Hetland<sup>3</sup> and Mark Simons<sup>2</sup>

<sup>1</sup>Jet Propulsion Laboratory, California Institute of Technology, Pasadena, CA 91109, USA. E-mail: zliu@jpl.nasa.gov

<sup>2</sup>Division of Geological and Planetary Sciences, California Institute of Technology, Pasadena, CA 91125, USA

<sup>3</sup>Department of Geological Sciences, University of Michigan, Ann Arbor, MI 48109, USA

Accepted 2010 March 14. Received 2010 February 27; in original form 2009 July 7

## SUMMARY

We model the crustal deformation caused by two long-term subduction slip transients in southwest Japan, which we refer to as the 2000–2004 Tokai and the 2002–2004 Bungo Channel slow slip events (SSEs). We use re-analysed GEONET position time-series, and a Kalman filter based network inversion method to image the spatiotemporal slip variation of the two events on the plate interface during the period of 1998–2004.67 and 2000–2005. Both events are found to have complex slip histories with multiple subevents. In addition to a newly identified slip subevent in 2002–2003, we find that the major event in the Bungo Channel SSE initiated in early 2003 beneath the northeastern corner of the region and expanded southwestward, in contrast to the slip characteristics suggested by other studies. The re-analysed GPS data in the Tokai region shows a renewed slip activity for the Tokai SSE in early 2003–2004 at a similar location as in the period of 2001–2002. The equivalent  $M_w$  for both the Tokai and Bungo Channel SSEs are about 7.0. Our results show that the Tokai SSE appears to start before the Miyaki-Kozu seismovolcanic event. Integrating plate coupling and SSEs shows that the transient slip zones are located in a region between the locked zones and the epicentres of the low frequency earthquakes (LFEs). At least part of the interseismic slip deficit is released by episodic SSEs beneath the Bungo Channel region. We find excellent temporal correspondence between transient slip and adjacent LFEs for both SSE, suggesting that they are closely related and possibly reflect that long-term slow slip may modulate the occurrence of LFEs.

**Key words:** Time-series analysis; Transient deformation; Subduction zone processes.

## 1 INTRODUCTION

Japan is one of the prime places to study ongoing crustal deformation and subduction zone dynamics. In southwest Japan (Fig. 1) the Philippine Sea Plate is subducting beneath the Amurian Plate at an annual rate of  $\sim 60\text{--}70\text{ mm yr}^{-1}$ , causing  $M \sim 8$  earthquakes every 100–200 yr over the past 1000 yr (e.g. Heki *et al.* 1999; Hori *et al.* 2004). Recently, thanks to the deployment of a dense continuous GPS network (GEONET) and a high-sensitivity seismograph network (Hi-net), a wide range of slow earthquake phenomena including long- and short-term slow slip events (L-SSE and S-SSE), non-volcanic episodic tremors, and low/very-low frequency earthquakes (LFE and VLF) have been discovered in southwest Japan (e.g. Ozawa *et al.* 2002, 2007; Hirose & Obara 2005; Ito *et al.* 2007). Here we use L-SSE to refer to SSE with durations of months to years, and we use S-SSE to refer to events with durations of days. Seismic tremors, LFEs, and VLFs occur over shorter time periods than S-SSEs, with VLFs having durations of hours to days. We collectively refer to seismic tremor, LFE, VLF and S-SSE as

‘short-term slow earthquakes’, which are in contrast to the much longer phenomena of L-SSE. Unless otherwise noted, we use both ‘transient slip’ or ‘slow slip’ to refer to the slip that appears in a SSE.

SSE have now been observed worldwide, with observations in Japan (e.g. Hirose *et al.* 1999; Ozawa *et al.* 2002, 2003, 2007; Sagiya 2004; Hirose & Obara 2005, 2006; Miyazaki *et al.* 2006; Heki & Kataoka 2008), Cascadia, Pacific Northwest (e.g. Dragert *et al.* 2001, 2004), Parkfield, central California (Murray & Segall 2005), Guerrero, southern Mexico (e.g. Lowry *et al.* 2001; Kostoglodov *et al.* 2003), Alaska (Ohta *et al.* 2006; Peterson & Christensen 2009), New Zealand (Douglas *et al.* 2005; Wallace & Beavan 2006; Beavan *et al.* 2007; McCaffrey *et al.* 2008), Hawaii (Cervelli *et al.* 2002; Brooks *et al.* 2006; Montgomery-Brown *et al.* 2009) and Costa Rica (Schwartz *et al.* 2008). Most SSE occur repeatedly at a variety of depths over durations of days to years. In subduction zones SSEs appear to occur within a transition region of frictional properties, from velocity weakening regions (seismic) at shallow depths to velocity strengthening regions (aseismic) deeper

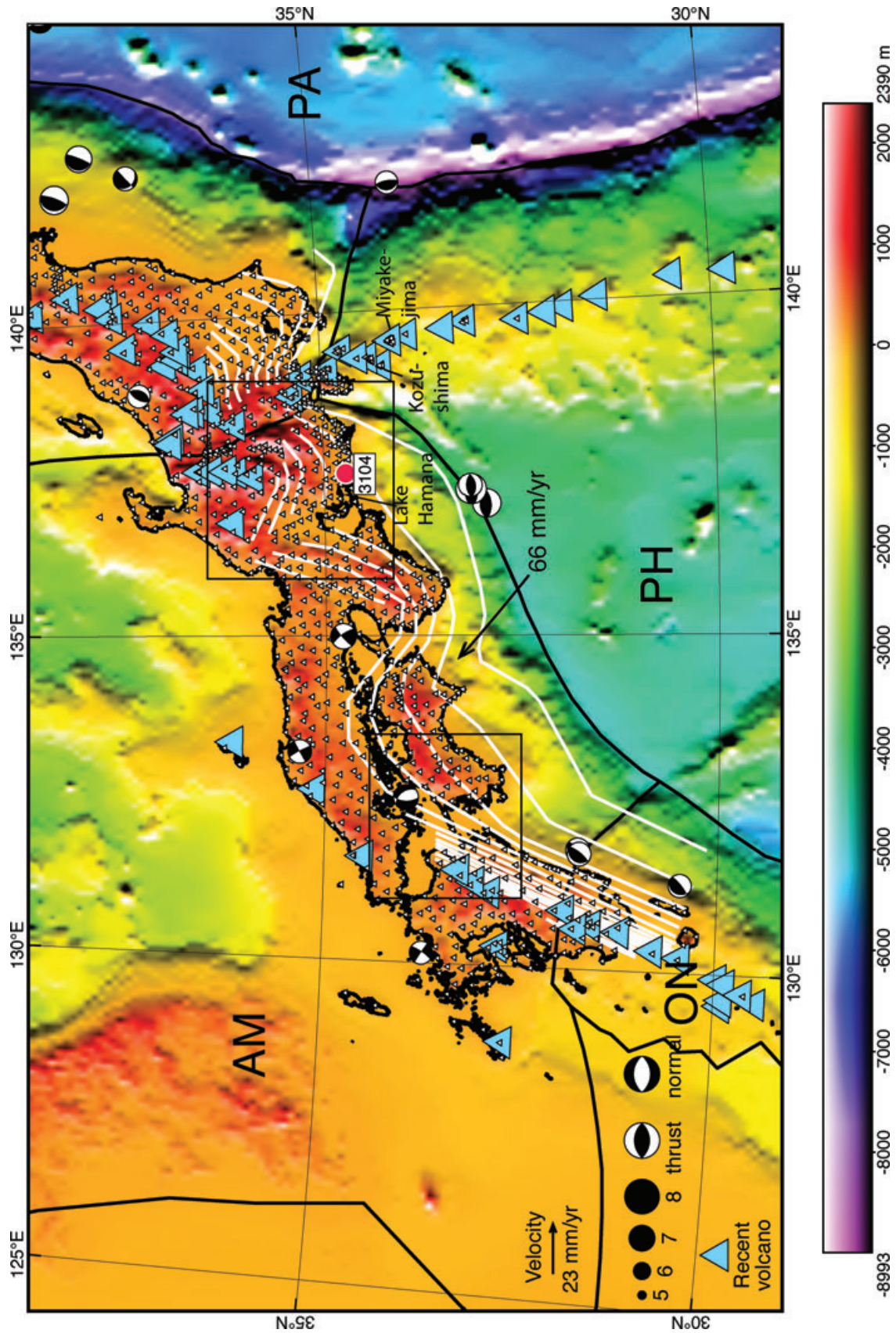


**Figure 1.** Regional tectonic map of southwest Japan. Colormap is the topography from ETOPO5. Focal mechanisms are shown for earthquakes in Global CMT with  $M_w > 6$  in 1996–2006 and depth range of 0–70 km. Relative motion between Philippine Sea Plate and Amurian Plate is indicated by the arrow. Cyan triangles represent active volcanoes. White lines represent the iso-depth contours of the upper surface of the Philippine Sea Plate. GPS stations in GEONET are indicated by black triangles. Two boxes show the locations where two long-term slow slip events occur. The station (3104) whose position time-series is shown in Fig. 2 is indicated. AM, Amurian Plate; PH, Philippine Sea Plate; PA, Pacific Plate; Miyake-jima and Kozushima are islands where Miyake-Kozu seismicvolcanic events occurred.

along the plate interface (Schwartz & Rokosky 2007). Several studies have noted a correlation between SSEs and tremor. For example, a relationship between SSEs and tremor has been well established in Cascadia and southwest Japan (e.g. Obara & Hirose 2006). A similar correlation between SSEs and tremor may also exist in Alaska (Peterson & Christensen 2009) and Mexico (Payero *et al.* 2008). SSE and tremor are not always linked, for example, in Hawaii and New Zealand, repeating SSEs are accompanied by microseismicity but not any detectible tremor (Segall *et al.* 2006; Delahaye *et al.* 2009; Montgomery-Brown *et al.* 2009). In southwest Japan, there is a strong coincidence between S-SSEs, tremor, LFE and VLF (Ito *et al.* 2007). Repeating occurrences of short- and long-term SSEs are also accompanied by deep tremor activity around the Bungo Channel region (Hirose & Obara 2005). The 2002–2004 Bungo Channel L-SSE was coincident with an increase of LFEs (Ozawa *et al.* 2007). In the Tokai region, despite a correlation between short-term slow slip episodes and tremor (Hirose & Obara 2006), any evidence for a correlation between long-term slow slip and LFE or seismic tremor is still lacking (Ozawa *et al.* 2005). More recently, a series of studies have illustrated that the short-term slow earthquakes (S-SSE, episodic tremor, LFE and VLF) are likely interconnected in space, and time and may represent different manifestations of a single process (e.g. Shelly *et al.* 2006, 2007a,b; Ide *et al.* 2007b, 2008; Ito *et al.* 2007). It is unclear how these short-term transients relate to interseismic plate loading and L-SSEs. Transient slip on the subduction interface can load adjacent locked portions of the megathrust, and may increase the probability of future large earthquakes in those regions (Linde & Sacks 2002). Alternatively, transient slip may delay earthquake timing by releasing accumulated elastic strain in the anticipated rupture zones (Roeloffs 2006). It is therefore crucial to have a better understanding of transient slow-slip phenomena and their relationship with plate loading process.

Since its inception, GEONET has captured several L-SSEs beneath the Bungo Channel and Tokai region (e.g. Hirose *et al.* 1999; Ozawa *et al.* 2004, 2005, 2007; Miyazaki *et al.* 2006). Ozawa *et al.* (2004, 2007) estimated the slip history of the Bungo Channel SSEs during 1996–1998 and 2002–2004 using GPS position time-series processed by the Geographical Survey Institute of Japan (GSI), which was based on a subnetwork analysis, and a square root information filter. Their modelling assumed a GPS reference frame with regard to a fixed fiducial site and did not use the variance-covariance matrices of the GPS solutions in their inversion for fault slip. They found that the L-SSEs in 1996–1998 and 2002–2004 were very similar in their source areas and moment magnitudes, but each with a distinct spatiotemporal evolution of slip. The 1996–1998 event started beneath the southwestern part of the Shikoku island and propagated southwestward to the Bungo Channel area, while 2002–2004 event initiated in the area beneath the Bungo Channel and during 2003 August–2004 January propagated northeastward to the southwestern edge of the Shikoku island (Ozawa *et al.* 2007). For the 2002–2004 event, Ozawa *et al.* (2007) revealed a coincidence between the sharp increase of aseismic slip and a rapid increase of LFEs during 2003 August–2004 January, with the LFEs occurring downdip of the region undergoing transient slip. However, they were not able to demonstrate a long-term correlation between aseismic slip and LFEs, partly due to a lack of correlation between the slip and LFEs before 2003 August. Using the same methodology, Ozawa *et al.* (2002, 2005) also inferred the slip history for the Tokai SSE up to 2004 May. They found that the transient slip was centred downdip and adjacent to the region of an anticipated Tokai earthquake. From 2002 there was an increase in relative slip towards the northeast and north of Lake Hamana. Miyazaki *et al.* (2006) decon-

strained the GSI overly constrained GPS solution, and recombined the position time-series from 2000 January to 2002 November. They then imaged the slip evolution in the early stage of the Tokai SSE, identifying two slip subevents. Based on the inverted slip history they suggested that the Tokai SSE may have initiated before the start of Miyaki-Kozu volcanic eruption, although there was large uncertainty associated with their resolved slip prior to the volcanic event. The accumulated slip in their model was located at a depth of ~25 km in the transition zone from the locked seismogenic portion of the megathrust to a freely sliding zone at depth. For the Tokai SSE, none of these studies identified a clear correlation between L-SSE and adjacent LFE/tremor.

A revisit to the slip transients in Japan is warranted for several reasons. First, we have re-analysed GPS data for the entire GEONET using a new network processing strategy and consistent time-series analysis framework (Liu *et al.* 2010). The improved processing has resulted in high precision GPS positions without fixing any fiducial sites, as compared to the solutions used in most previous studies. The new time-series prompts a further investigation of these L-SSEs. Second, the Tokai slow slip event appears to affect surface GPS stations in a broader region than previously shown. Previous studies have used either limited station coverage or a limited data period to infer transient slip. For example, Miyazaki *et al.* (2006) only used data from 2000 January to 2002 November, while Ozawa *et al.* (2004) used a longer data window (2000 September–2004 May) but with a very limited station distribution. In this study, we use ~6 yr of position time-series (1998.0–2004.67) and include sites in a broader spatial range. Third, we are interested in examining the relationship between the slow earthquake phenomena (e.g. LFEs) and the longer-term SSE in the Tokai and Bungo Channel region, southwest Japan. Interesting correlations have been noted among the short-term slow earthquake phenomena (e.g. tremor, LFE, VLF and S-SSE) (e.g. Obara *et al.* 2004; Hirose & Obara 2006; Obara & Hirose 2006; Shelly *et al.* 2006, 2007a,b; Ide *et al.* 2007b; Ito *et al.* 2007) and between SSEs (e.g. Hirose & Obara 2005; Ozawa *et al.* 2007). For example, non-volcanic tremors seem to consist of a sequence of LFEs that can be attributed to fluid-enabled shear slip on the plate interface (Shelly *et al.* 2006, 2007a,b; Ide *et al.* 2007b). There is remarkable spatiotemporal coincidence between tremors, LFE, VLF and S-SSEs in Japan (Obara *et al.* 2004; Hirose & Obara 2006; Obara & Hirose 2006; Ito *et al.* 2007). However, a quantitative assessment of the spatiotemporal correlation between both Bungo Channel and Tokai L-SSE and LFEs has not yet been established. Additionally, Ide *et al.* (2007a) recently proposed that slow earthquakes, regardless of their size and duration, satisfy a unified scaling law between moment and duration. We will use the newly estimated slip and moment for the Bungo Channel and Tokai L-SSEs to see if these L-SSEs follow the same scaling relationship since their duration and moment differ by several orders of magnitude from the shorter-term phenomena such as tremor and S-SSEs. Finally, we have made an improved estimate of plate coupling in southwest Japan using three-component GPS velocities derived from the same GPS time-series used to estimate the transient events (Liu *et al.* 2010). This allows for an integrated study of aseismic slip transient, LFEs/tremors, and plate coupling that is valuable in understanding the relationship between these transient slip events and the steady plate loading process, which has implications for understanding earthquake hazard in this part of the plate boundary.

Here we use the re-analysed GPS data to model the space-time slip variation for both Bungo Channel and Tokai SSEs. We refer to the Bungo Channel event as the 2002–2004 Bungo Channel SSE

to reflect the time of major slip activity. Our inversion method is an extended Network Inversion Filter (ENIF) (McGuire & Segall 2003), which is based on an extended Kalman filter but modified to include complex interplate fault geometry. For the Bungo Channel SSE, we use 2000–2005 for the time period of analysis to resolve subtle slip subevents in addition to the major slow slip activity in 2003–2004. For the Tokai SSE, we model data from 1998 to 2004.67, and our analysis includes more GPS sites and longer time-series than used in prior analysis. We examine the space–time slip evolution for both events and their spatiotemporal relation to LFEs. We revisit the issue of whether the Tokai slow slip event initiated before the Miyake-Kozu volcanic eruption, and provide improved estimates of slip uncertainties. Finally, we integrate inferred transient slip with the interseismic plate coupling model developed in a companion study (Liu *et al.* 2010) to examine the slip budget on the subduction megathrust, and we discuss the implication for future earthquakes.

## 2 GPS DATA

We processed continuous GPS data in the period of 1996–2006 for all of the GEONET stations (Liu *et al.* 2010). We used a distributed processing strategy, based on the GIPSY-OASIS software, which avoids the use of subnetworks and allows for efficient processing of bias-fixed solutions for large networks. The details about the data processing and analysis procedure are described in a companion study (Liu *et al.* 2010). Using this data analysis, we obtained high precision east, north, up position time-series for > 1200 GPS stations in the ITRF2000 reference frame. We developed sets of customized

time-series analysis tools which can estimate bias, offsets caused by instrument changes, earthquakes and other unknown sources, linear trends, seasonal variations, post-seismic deformation and other transient signals. The principal component analysis (PCA) method was used to estimate the common mode error (CME) across the network (Dong *et al.* 2006). We then use the cleaned position time-series that have been corrected for CME to infer plate coupling and estimate transient slip during the SSEs. Fig. 2 shows the time-series of site 3104 before and after the removal of the CME. Removing CME reduces the scatter in the raw ENU time-series and enhances the signal-to-noise ratio of the remaining time-series.

## 3 MODELLING METHOD

We apply an extended network inversion filter (ENIF) (McGuire & Segall 2003) to model time variable deformation signals. The network inversion filter is based on a Kalman filter and is able to distinguish spatially coherent signals, such as transient fault slip, from incoherent motions due to non-tectonic sources (e.g. local benchmark motions). Derived from the original network inversion filter (Segall & Matthews 1997), the ENIF allows us to include temporal and spatial smoothing parameters in the state vector. The filter and its various versions have been used to study post-seismic slip as well as aseismic slip transients in different tectonic settings (e.g. Segall *et al.* 2000; Burgmann *et al.* 2002; Murray & Segall 2005; Miyazaki *et al.* 2006; Hsu *et al.* 2007).

We used the time-series analysis module in the Quasi-Observation Combination Analysis (QOCA) software (available at <http://gipsy.jpl.nasa.gov/qoca>) (Dong *et al.* 1998) to remove

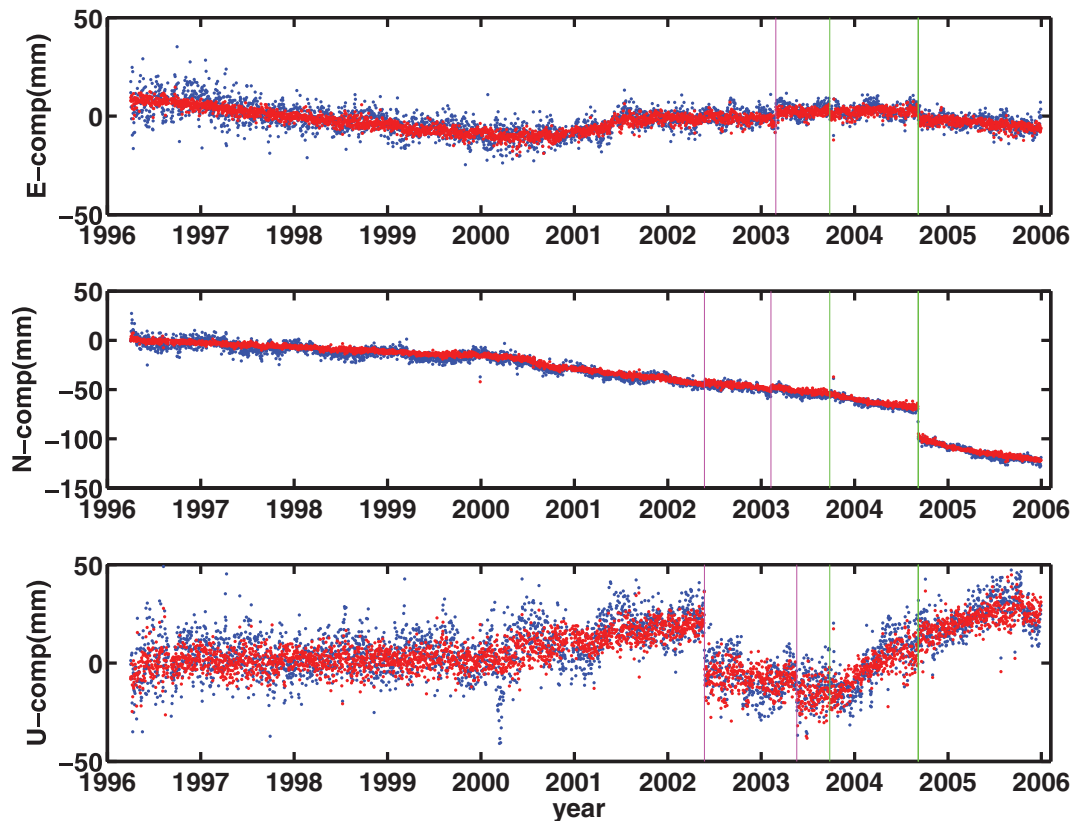


**Figure 2.** Raw E, N and U position time-series (blue dots) versus cleaned ones (red dots) for station 3104. Offsets are indicated by colour lines. Green – earthquake related offsets. Magenta – offsets due to instrument changes or unknown causes.

seasonal variations and correct offsets. The resulting time-dependent GPS station positions,  $X(t)$ , are modelled with the following equation:

$$X(t) = V \bullet (t - t_0) + \int_A S_p(\xi, t - t_0) G_{pq}^r(x, \xi) n_q(\xi) dA(\xi) + Ff(t) + L(x, t - t_0) + \varepsilon,$$

where the first term on the right hand side represents a steady-state velocity field.  $S_p(\xi, t - t_0)$  is the time-dependent slip on the faults as a function of position  $\xi$ , which is related to the site position through the Green's functions  $G_{pq}^r$ .  $S_p$  represents only the transient component of fault slip. The Green's functions relating slip to surface displacement can be computed using analytical expressions for dislocations in uniform elastic half-spaces, although there is no impediment to computing Green's functions in heterogeneous or layered media. Here  $p, q$  and  $r = 1, 2$  and  $3$ , and summation on repeated indices is implied, and  $n_q(\xi)$  is the unit normal to the fault surface  $A(\xi)$ .  $Ff(t)$  represents reference frame error and  $L(x, t - t_0)$  represents random benchmark wobble. Measurement error,  $\varepsilon(t)$ , is assumed to follow a normal distribution with zero mean and covariance  $\sigma^2 \Sigma(t)$ , where  $\Sigma(t)$  is the covariance matrix of GPS positions and  $\sigma^2$  is a scale factor to account for unmodelled errors in GPS data processing.

The traditional ENIF works only on rectangular fault surfaces, which fails to account for the complexity of fault geometry. Here we use the extension of the filter that relies on a triangular-mesh fault surface, and can better represent complex 3-D fault surfaces (Liu & Segall 2006). We use an interplate fault geometry from a composite plate boundary model (Wang *et al.* 2004). Comparison with different fault geometries, such as that proposed by Nakajima & Hasegawa (2007), suggests that different plate boundary fault geometries do not have much influence on estimated slip distributions (Liu *et al.* 2010). All fault surfaces are constructed from discrete iso-depth contour points in the composite plate boundary model of Wang *et al.* (2004) by applying point/boundary constraints and isotropic discrete smoothing interpolation (Mallet 1989). We compute the elastostatic Green's function  $G_{pq}^r$  using triangular dislocation elements (Jeyakumaran *et al.* 1992). Spatial smoothing on a triangular surface is based on the Fujiwara operator (Desbrun *et al.* 1999) and computed as  $\nabla^2 m_i = \frac{2}{L_i} \sum_{j=1}^3 \frac{m_j - m_i}{h_{ij}}$ , where  $m_i$  represents the average slip (or slip rate) of the  $i$ th fault element,  $h_{ij}$  is the distance between element  $i$  and its adjacent element  $j$  and  $L_i = \sum_{j=1}^3 h_{ij}$ .

## 4 MODELLING AND RESULTS

We assume that transient deformation observed at the surface results from the slip on the interplate subduction megathrust. We apply the ENIF described above to image spatiotemporal fault slip distribution for the Bungo Channel SSE and the Tokai SSE. As discussed in the introduction, while significant transient deformation occurs in 2002–2004 for the Bungo Channel event and 2000–2004.67 for the Tokai event, we use a longer time span in the inversion for each event (2000.0–2005.0 for Bungo Channel and 1998–2004.67 for Tokai). This ensures the filtering results are not biased by the *a priori* zero slip constraint imposed at the beginning of each modelling period. We constrain slip to be zero at the edges of each modelled fault boundary and we impose non-negative constraints so that dip-slip and strike-slip components are to the south and east, respectively. Such constraints assume that the slip transient on the plate interface

moves roughly in the direction opposite to the relative PH-AM plate convergence.

### 4.1 Time-dependent inversion of 2002–2004 Bungo Channel slow slip event

#### 4.1.1 Slip in space and time

We use the continuous position time-series of 58 selected stations to estimate the transient slip beneath the Bungo Channel region over the period of 2002–2005 (Fig. 3). We select the stations that have high signal-noise ratios based on a visual inspection of the position time-series. We weight the east, north, and up components based on their standard deviation, and in this case the weighting ratio between east, north and up is about 1:1:1/3. As described earlier, we remove seasonal variations and corrected offsets due to earthquakes, instrument changes, and other unknown causes. We estimate a linear deformation rate for the period of 2000–2002.0 by assuming the rate is constant and that the large aseismic slip that initiated in 2002 would not affect this linear rate. We then use these secular rate estimates as *a priori* site velocities. We impose a tight constraint of  $\sim 1 \text{ mm yr}^{-1}$  on the final velocity estimates in the filtering process. We estimate the total displacement caused by the SSE by subtracting the position predicted using the 2000–2002 linear rate from the mean observed position in 2004.8–2005.0 (Fig. 3). Most GPS sites move southeastward in the SSE, consistent with the assumption that transient slow slip occurs in a direction opposite to the PH-AM relative motion.

The total transient slip in the Bungo Channel SSE in the period of 2002–2005 has a maximum slip of  $\sim 260 \text{ mm}$  (Fig. 4). The maximum slip uncertainty inferred from state vector covariance in the filter output is  $\sim 16 \text{ mm}$ , and it is larger at deeper depths ( $> 30 \text{ km}$ ) compared to shallower depths ( $< 20 \text{ km}$ ). The total moment estimate for this SSE is  $\sim 3.46 \times 10^{19} \text{ N m}$  assuming a shear modulus of  $30 \text{ GPa}$ , equivalent to a  $M_w$  of  $\sim 7.0$ , with an average stress drop of  $\sim 0.08 \text{ MPa}$ . Slip vectors projected on the surface point to the southeast, which is consistent with the GPS observations. LFE epicentres are located at the downdip edge of the slip locus area, consistent with previous studies (Ozawa *et al.* 2007) and indicate a potential causal relationship between the L-SSE and LFEs.

The predicted position time-series from our model of the transient slip in the Bungo Channel SSE are a good fit to the GPS time-series for all three components (Fig. 5). Using the ENIF approach, we also obtain the slip evolution with time (Fig. 6). Each panel in Fig. 6 represents a snapshot of the incremental slip over an interval of 42 d on the projected fault surface. The maximum incremental slip is up to  $47 \text{ mm}$ , and slip uncertainties do not exceed  $\sim 5.2 \text{ mm}$ . Two slip subevents are apparent, with the first subevent initiating in early 2002.0 beneath the southwest corner of the Bungo Channel region. Slip during this subevent gradually increases to a maximum of  $\sim 19 \text{ mm}$  by  $\sim 2002.58$ , and then wanes to insignificant levels by late 2002. The locus of slip in this subevent is relatively stationary in space. The second subevent initiates beneath the northeast corner of the Bungo Channel in early 2003, expanding southwestward and reaching a peak slip of  $\sim 47 \text{ mm}$  during the 2003.73–2003.84 interval. Transient slip in the second subevent begins to subside after  $\sim 2003.9$ , with fault slip returning to pre-slip levels by about mid-2004.

Ozawa *et al.* (2007) compared the 1996–1998 and 2002–2004 SSEs in the Bungo Channel, finding that both events occurred in about the same area and had similar moment release. However,

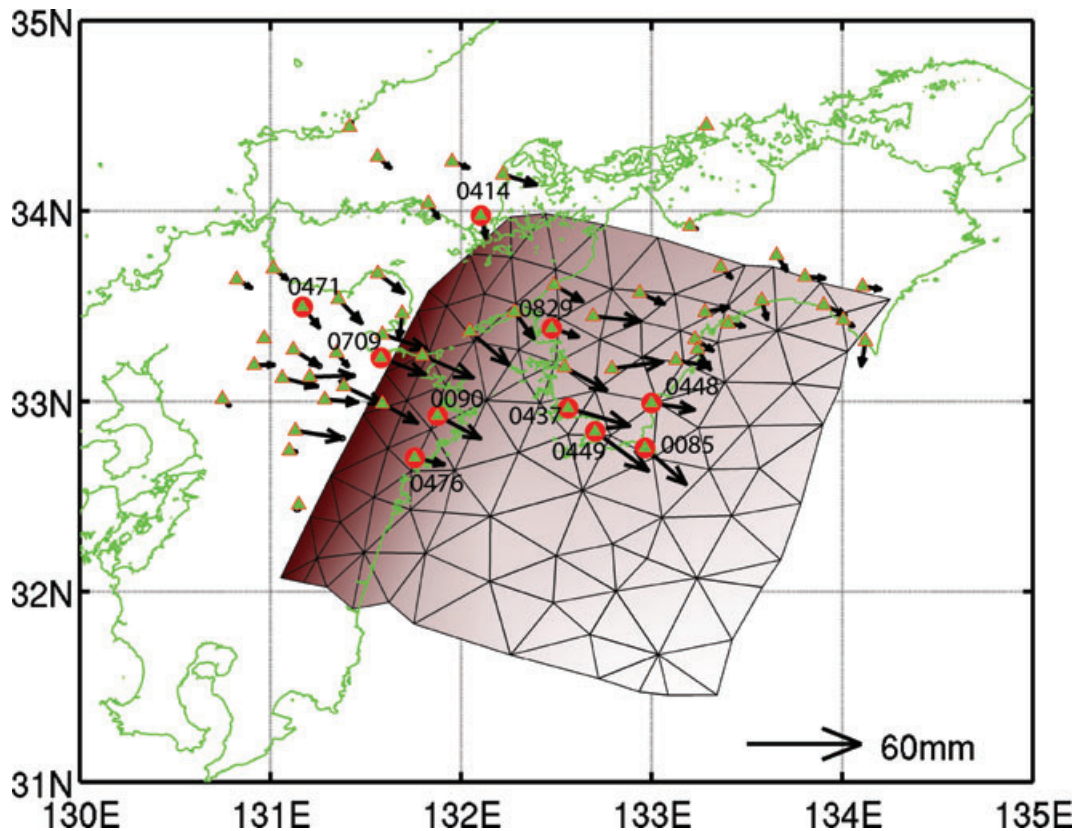


**Figure 3.** Mapview of the total displacements in the 2002–2004 Bungo Channel slow slip event. The displacement is calculated by subtracting projected position using rate estimate of 2000–2002 from the mean position in 2004.8–2005.0. Red filled circles with names are stations whose time-series and model fit are shown in Fig. 5.

they inferred that the 1996–1998 SSE initiated beneath the north-east corner of the region and expanded to the southwest, while the 2002–2004 SSE expanded northeastward onto a deeper area of the fault compared to the early slip of the SSE. In comparison, the major subevent in our study appears to have initiated at  $\sim 2003.15$  with transient slip propagating to the southwest, which contrasts the spatiotemporal pattern of transient slip in the 2002–2004 SSE in the model of Ozawa *et al.* (2007), but roughly consistent with the transient slip in the 1996–1998 SSE inferred by Ozawa *et al.* (2001).

The total moment release in the Bungo Channel SSE during 2002–2004.5 is dominated by the 2003–2004.5 slip subevent, which alone accounts for  $\sim 74$  per cent of total moment release (Figs 6 and 7a). The moment in the 2002–2003 subevent is  $\sim 1.02 \times 10^{19}$  N m ( $M_w \sim 6.6$ ). There is an earlier subevent in the Bungo Channel region during 2001–2002 (Figs 7a and b), whose moment is about  $\sim 2.43 \times 10^{18}$  N m ( $M_w \sim 6.2$ ). It is unknown what is the smallest transient slip event at depth that can be resolved by a dense GPS network. In the Cascadia subduction zone, decade-long GPS observations are able to resolve SSEs with  $M_w > 6.3$  (Szeliga *et al.* 2008). Here we find a similar detection limit, with  $M_w$  in the 2001–2002 subevent as low as  $\sim 6.2$ .

#### 4.1.2 Relationship between the Bungo Channel slow slip and LFEs

We examine the spatiotemporal relationship between the Bungo Channel L-SSE and LFEs (Figs 7a and b). LFEs are relatively energetic isolated pulses with identifiable *S*-wave arrivals in low-

frequency tremor wave trains (Shelly *et al.* 2007a). The Japan Meteorological Agency (JMA) routinely identifies LFEs and publishes them in their online catalogue. Tremor seems to consist of a sequence of LFEs and occur concurrently with 20 s-period VLF earthquakes (Shelly *et al.* 2007a; Ito *et al.* 2007). Identifiable phases in LFE improve the determination of their focal mechanism and location error, compared to those determined using emerging tremor signals (Matsubara *et al.* 2009). The spatio-temporal coincidence between tremor, LFEs and geodetically observed short-term SSE suggest that they may be the manifestations of the same process, possibly shear slip on the plate interface (e.g. Hirose & Obara 2005, 2006; Wech & Creager 2007; Ide *et al.* 2008). Fig. 7 shows the temporal variation of transient slip and slip rate in the fault patch corresponding to the maximum slip in the Bungo Channel SSE compared to number of LFEs within a slightly larger region (see Fig. 4 for the location of the fault patch and the region of LFEs). The average slip and slip rate at all fault patches within the circle show a similar temporal variation as those in the selected fault patch. Both long-term transient slip and slip rate display an excellent temporal correspondence with LFEs, despite the less smooth pattern of the LFEs. The increase in transient slip from 2002.5 to 2003.0 is accompanied by an increase in LFEs during the same period. A significant increase in the slip also occurs around 2003.2, with a correspondingly large increase in LFE activity. The number of LFEs decreased at  $\sim 2004.5$ , coincident with the cessation of transient slip. The remarkable correspondence between the Bungo Channel SSE and LFEs suggests that transient fault slip and LFEs are temporally correlated, similar to the temporal correspondence between long-term slow slip and microseismicity

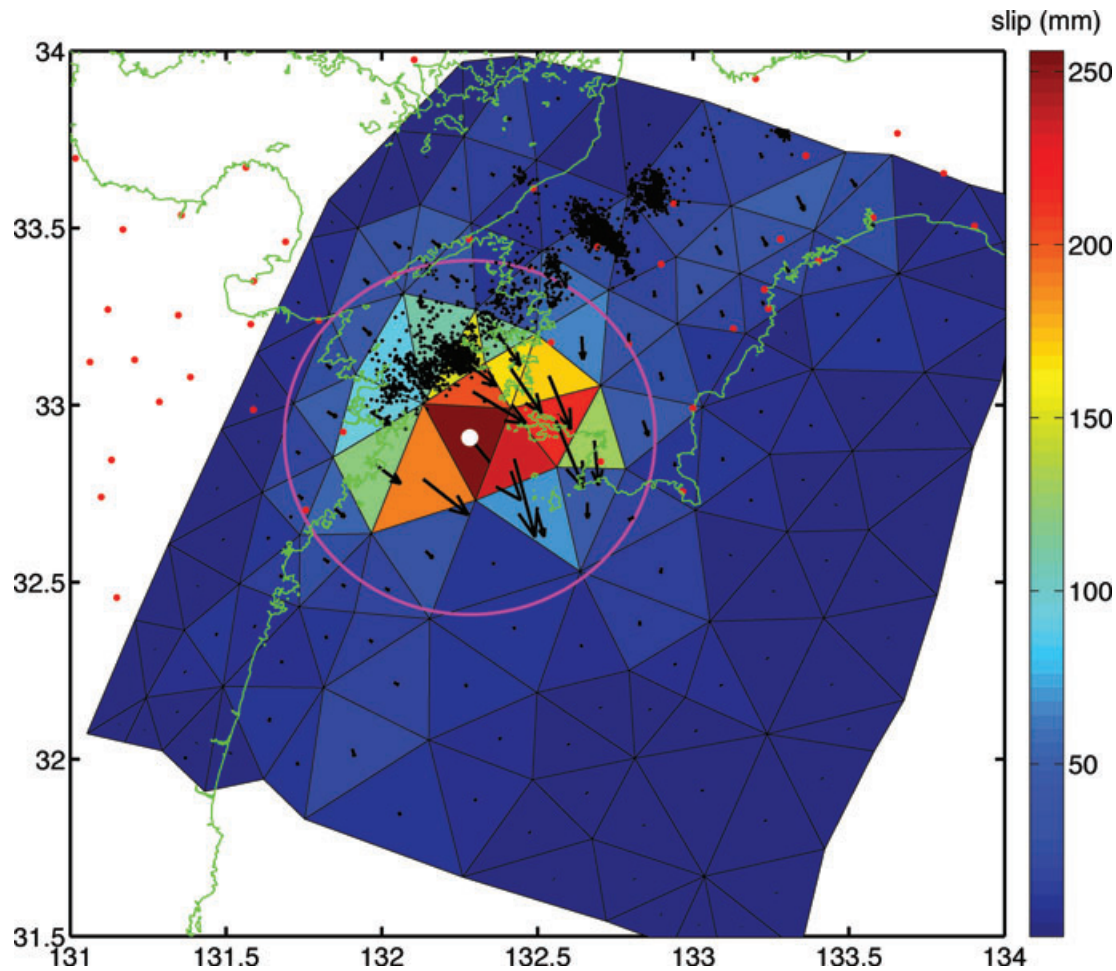


**Figure 4.** Total slip in the 2002–2004 Bungo Channel slow slip event (SSE). Also overlaid are the epicentres of low frequency earthquakes (LFEs) from JMA. Black arrows are projected slip vectors on the surface. Black dots are epicentres of LFEs. White dot indicates the fault patch with the maximum total slip, and the slip history of this selected patch is shown in Fig. 7. Circle indicates the region in which LFEs are considered in Fig. 7 (circle has radius  $0.5^\circ$  from the centre of the selected fault patch).

in the Hikurangi subduction zone, New Zealand (Delahaye *et al.* 2009).

Our results show that LFEs are concentrated at the downdip edge of the region of maximum transient slip (Fig. 4). This result has not changed when we use a finer-scale fault mesh. Typical location errors of LFEs are  $\sim 3$  km (Matsubara *et al.* 2009). There is a general agreement between LFE locations determined by JMA and relocated LFEs in western Shikoku during the period of 2002.5–2005.43 (David Shelly 2008, personal communication), suggesting that the JMA locations of the LFEs are fairly reliable. We also find similar spatial and temporal correlation between the Tokai L-SSE and LFEs, as discussed later, making it likely that these correlations hold in general for SSEs and LFEs along the southwest Japan trench.

## 4.2 Time-dependent inversion of the Tokai slow slip event

### 4.2.1 Slip in space and time

We next consider the spatiotemporal pattern of transient slip during the Tokai slow slip event using the data in 1998–2004.67. Previous studies have suggested that the Tokai SSE initiated in early 2000, and no significant slip transient inferred before 2000 (Miyazaki *et al.* 2006). We estimate the *a priori* steady state velocity using data from

1998 to 2000, and impose tight constraints on the final velocity estimates in the filter calculation. The 2004 September 5  $M_w > 7$  fore- and main shock sequence off the Kii Peninsula, a consequence of slab tensional bending and collision stress (Seno 2005), introduced widespread post-seismic deformation signals among stations in the Tokai region, so we only use data up to 2004.67 to avoid any effect from this earthquake sequence. We use 177 GPS sites in the Tokai region, and find that the Tokai SSE affects the surface deformation over a broader spatial extent than previously analysed (Fig. 8). We include more stations in the western Tokai area than previous studies (e.g. Ozawa *et al.* 2005; Miyazaki *et al.* 2006). However, we exclude stations in the eastern Tokai region, Izu Peninsula and Boso Peninsula, Miyake-jima and Kozu-shima Islands, as GPS stations in these regions are strongly affected by Miyake-Kozu seismovolcanic events that started on 2000 June 26. The locations of the selected stations are also consistent with the spatial characteristics of the Tokai SSE as revealed by the PCA of Kawamura & Yamaoka (2006). There were a large number of antenna changes at GPS stations in early 2003, and using the analysis strategy described above, we identified and corrected all of the associated offsets. The consistent slip pattern before and after early 2003 suggests that the instrument changes do not have much influence on the resultant fault slip estimates.

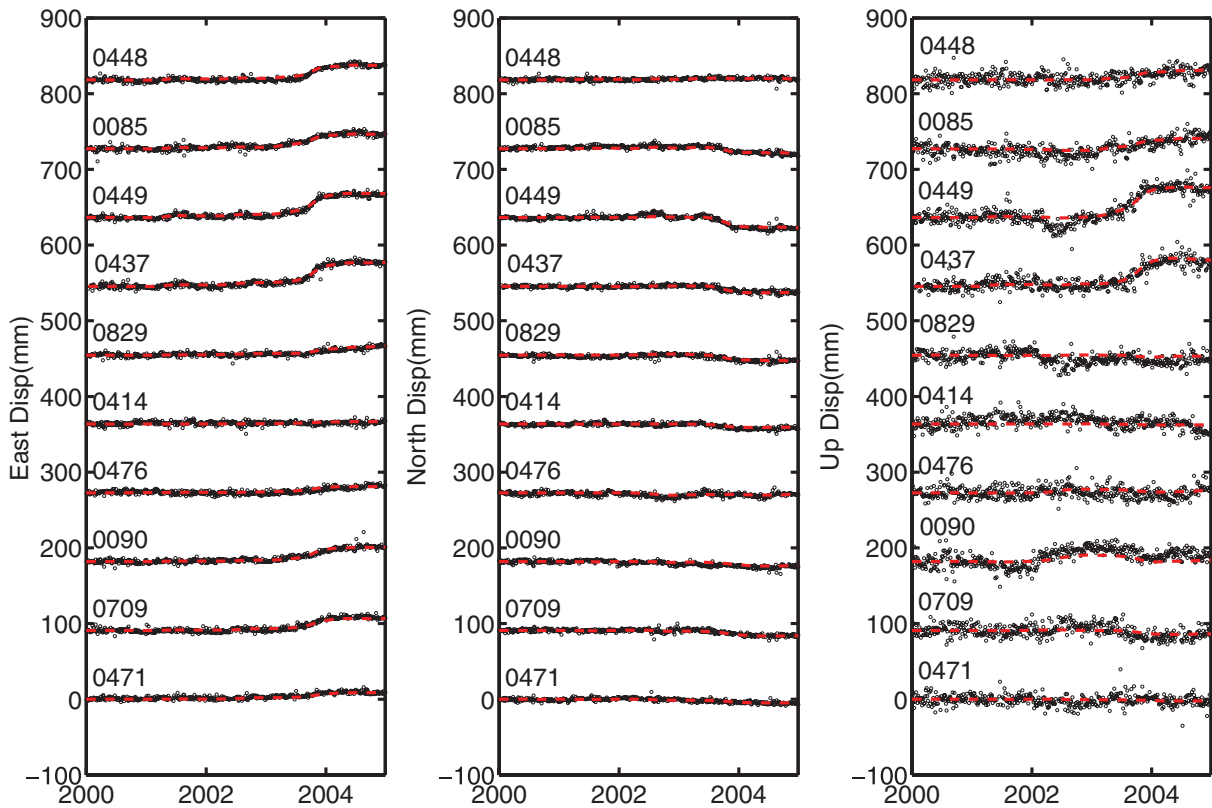


**Figure 5.** Predicted position time-series and the position time-series at selected GPS stations for the 2002–2004 Bungo Channel SSE. The station locations are indicated in Fig. 3. The data (black circles) have been corrected for reference frame error and a linear velocity, but contain benchmark wobble noise. The model prediction (dashed magenta line) is predicted displacement from the Bungo Channel transient slip model.

The total fault slip for the Tokai SSE during 2000–2004.67 is shown in Fig. 9. The maximum slip is  $\sim 240$  mm. Uncertainties in the estimated slip are less than  $\sim 7.4$  mm, and are generally smaller in the fault patches shallower than 20 km. The total moment released in the Tokai SSE is  $\sim 4.55 \times 10^{19}$  N m, equivalent to an earthquake of  $M_w \sim 7.04$ . The average stress drop is  $\sim 0.05$  MPa, similar to that in the Bungo Channel SSE. Stress drops in both the Tokai and Bungo Channel SSEs are about two orders of magnitude smaller than inferred stress drops in normal earthquakes (1–10 MPa). The region of maximum transient slip lies at the downdip edge of the fault region on which a future Tokai earthquake is anticipated (Central Disaster Management Council 2001).

The predicted position time-series from our model of transient slip during the Tokai SSE are a good fit to the observed time-series for all three components (Fig. 10). A similarly good fit was also obtained for other stations in the Tokai area but they are not shown here due to space limitation. The inferred spatiotemporal evolution of transient slip in the Tokai SSE is shown in Fig. 11. Each subplot of Fig. 11 represents a snapshot of slip rate at a 60 d interval. For clarity, uncertainties are not shown, but they are typically about  $5 \text{ mm yr}^{-1}$  with a maximum of  $\sim 15 \text{ mm yr}^{-1}$ . The slip rate is initially near zero in early 2000. This result is not influenced by *a priori* constraint, since we start analysis from 1998 and the zero *a priori* slip rate constraint imposed at the beginning has little effect on the slip in 2000. The slip rate starts to exceed the uncertainty level by about 2000.35, slightly before the Miyake-Kozu seismovolcanic event (2000 June 26 or 2000.4836). Transient slip appears to initiate to the east of Lake Hamana ( $\sim 137.5^\circ\text{E}$ ,  $34.7^\circ\text{N}$ ) in early 2000, then

accelerate and migrate slightly downdip. Slip develops around the Lake Hamana area in late 2000, and persists there until  $\sim 2001.8$ , reaching a maximum rate of  $\sim 60 \text{ mm yr}^{-1}$ . Starting in late 2001 the slip locus begins to migrate slightly downdip and towards the northeast. The transient slip subsides in late 2002, although another slip subevent initiates in late 2002 to early 2003 slightly north of Lake Hamana. The slip rate in the second subevent accelerates to  $\sim 100 \text{ mm yr}^{-1}$  in late 2003–early 2004 then gradually subsides after  $\sim 2004.2$ . At the end of the modelling period ( $\sim 2004.67$ ) transient slip is still persisting at rates of  $\sim 50\text{--}60 \text{ mm yr}^{-1}$ .

#### 4.2.2 Relation between the Tokai slow slip and the Miyake-Kozu seismovolcanic event

It is controversial whether the Miyake-Kozu seismovolcanic event may have triggered the Tokai slip transient, although both events occurred at nearly the same time (Schwartz & Rokosky 2007). Clarifying their relative timing is important for constraining possible mechanisms of the Tokai SSE. Miyazaki *et al.* (2006) suggested that the Tokai SSE might initiate before the onset of Miyake-Kozu seismovolcanic event. However, there was large uncertainty with their resolved slip before the volcanic event, which precluded a more robust conclusion. Due to the lower uncertainty in our estimate of early transient slip, we can investigate the relative timing by examining the slip history of two fault patches (Fig. 12, see Fig. 9 for the location of A, B). We focus on the forward filter solution, as back smoothing in the ENIF may smear the onset of the signal



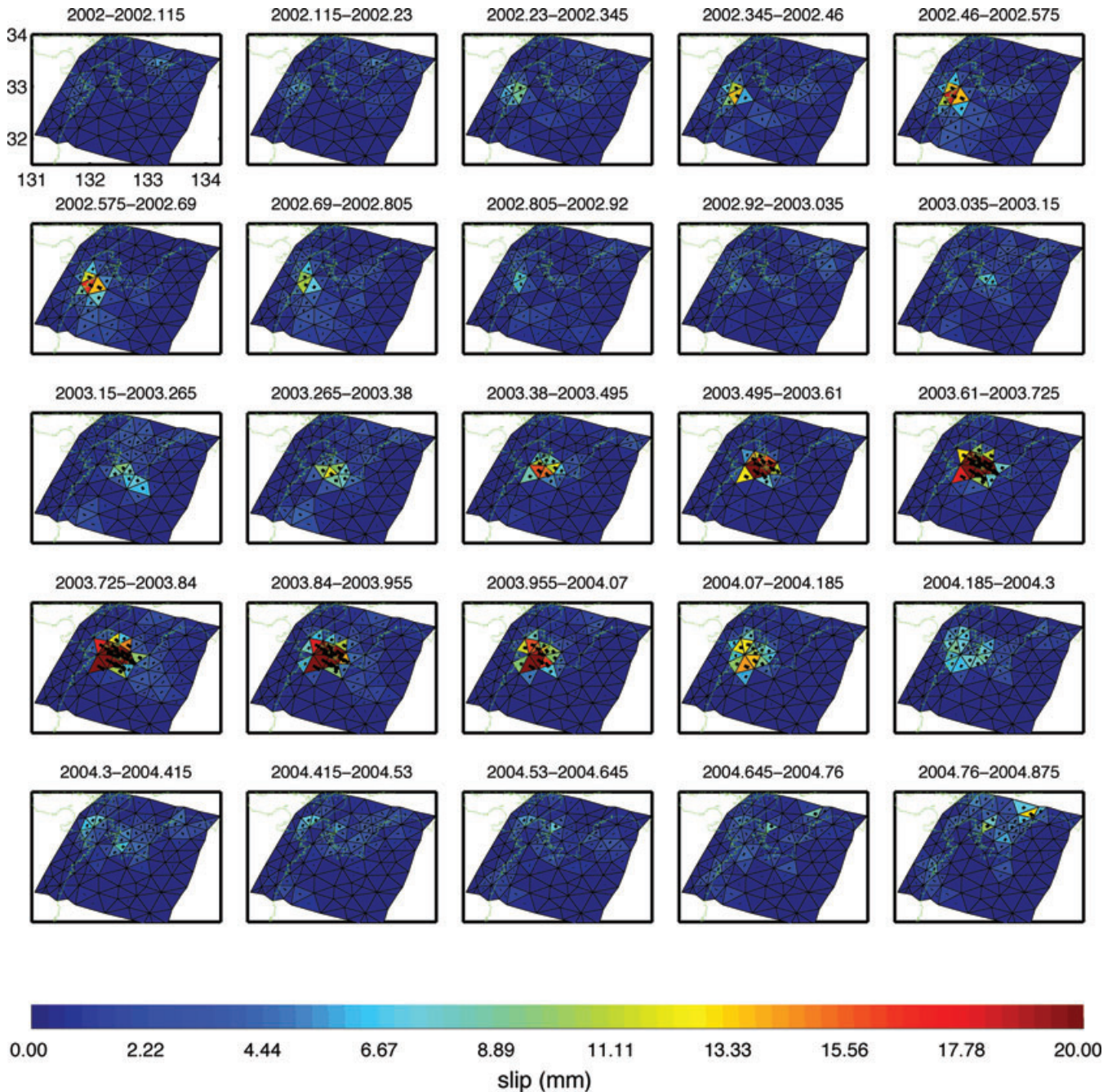


**Figure 6.** Space–time evolution of the transient slip for the 2002–2004 Bungo Channel slow slip event in the period of 2002–2005.0. Subplots represent the incremental slip at a time interval of 42 d. The subplot from 2004.85 to 2005.0 is not plotted because the time interval is less than 42 d. Colour scale is saturated at 20 mm to better reveal the details. Maximum incremental slip is  $\sim 47$  mm. Note that the slip unit is mm.

(Murray & Segall 2005). Both slip histories suggest that the slip starts to exceed the uncertainty level at  $\sim 2000.3$ , well before the onset of the Miyake-Kozi seismovolcanic event (Fig. 12a). The transient slip in the region that experiences most accumulated slip (patch A) is initially lower than the slip in the northeastern region of the fault (patch B), but it starts to exceed the slip at patch B after  $\sim 2001.2$  (Fig. 12b). This indicates that the slip initiates to the east of Lake Hamana and then starts to develop around Lake Hamana in late 2000–early 2001 and continues in the region of the main slow slip activity.

#### 4.2.3 Recurrent *L*-SSEs in the Tokai area

Several lines of observations suggest that the Tokai SSE may be recurrent. Historical baseline measurements from electromagnetic distance meter (EDM) surveys suggested that other similar SSE have occurred near the Tokai area in 1978–1983 and 1987–1991 (Kimata *et al.* 2003). If we assume the plate convergence rate is  $\sim 20\text{--}30$  mm yr $^{-1}$  in the Tokai region (Heki & Miyazaki 2001) and elapsed time since the last SSE is 9 yr, then the accumulated slip deficit is  $\sim 180\text{--}270$  mm. This is in rough balance with the total slip

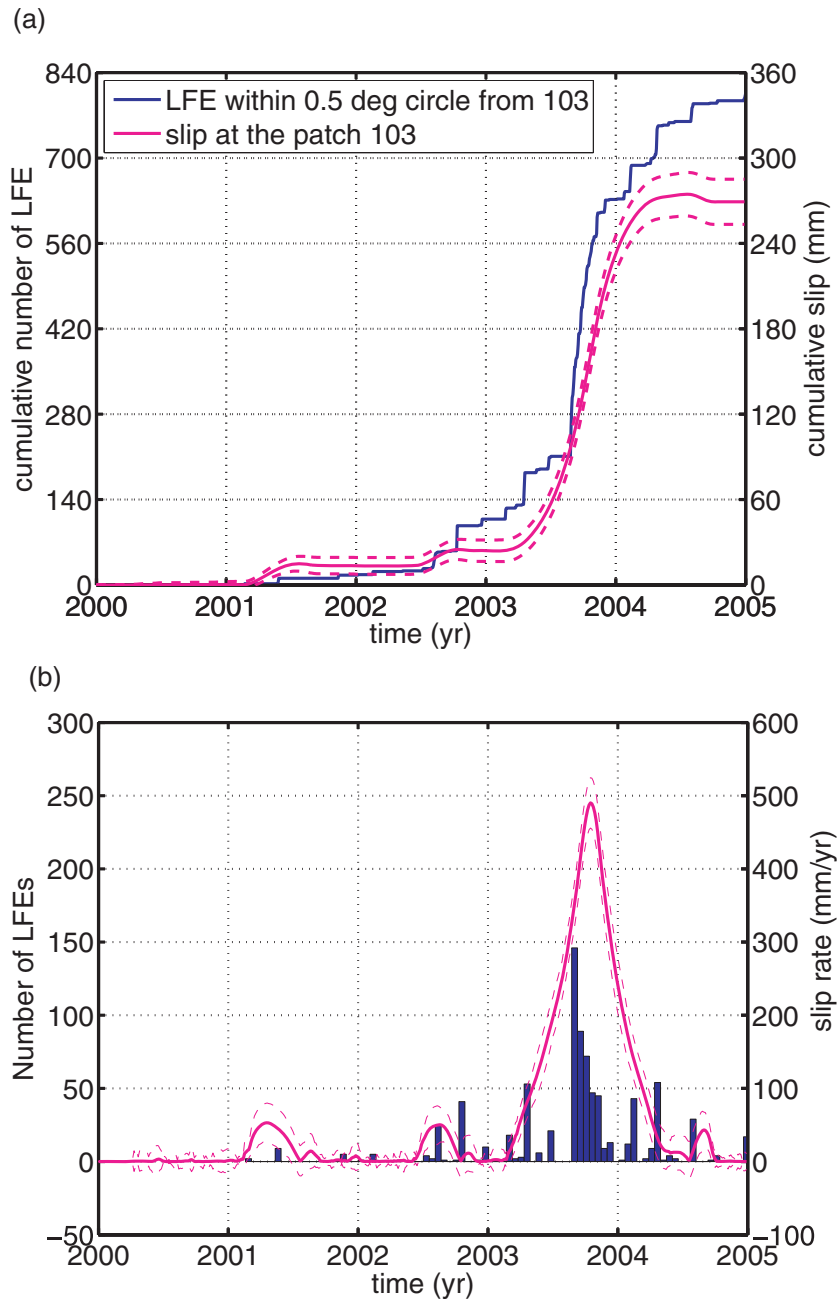


**Figure 7.** Temporal correlation between slip (a) and slip rate (b) at a selected fault patch (white dot in Fig. 4) and variation in low frequency earthquakes in the region depicted in Fig. 4. (a) Slip (magenta line) versus the cumulative count of LFEs (blue line). Dashed lines are  $1\sigma$  uncertainty bounds for the slip. (b) Slip rate (magenta line) versus distribution of the LFE occurrence. Dashed lines are  $1\sigma$  uncertainty bounds.

of  $\sim 240$  mm we estimate for the Tokai transient (Fig. 9), implying that long-term aseismic slip transients can release significant elastic strain energy accumulated in the transition zone.

#### 4.2.4 Relationship between the Tokai slow slip and LFEs

For the Tokai SSE, we observe the same spatial relationship between the transient slip and LFEs as was seen for the Bungo Channel SSE, and also in agreement with the previous model (Ozawa *et al.* 2005). The LFEs are predominantly located at the downdip edge of the region of large transient slip (Fig. 9). Similar to that in the Bungo

Channel SSE, we found a good correspondence between the temporal evolution of transient slip (and slip rate) and the occurrence of LFEs (Fig. 13). From early 2001 to mid-2002, and again in late 2002 to early 2004, increased transient slip is coincident with an increase in occurrence of LFEs. In mid-2002, the transient slip rate decreases, coincident with a relative quiescence of LFEs. The temporal correlation becomes less clear early in 2000, probably due to the sporadic LFEs at that time. In late 2004 there are some short times of increased occurrence of LFEs during a time when transient slip rate is relatively low. This may indicate some complex interactions between L-SSEs and LFEs, possibly due to other effects such as tidal loading or interactions with nearby S-SSEs with

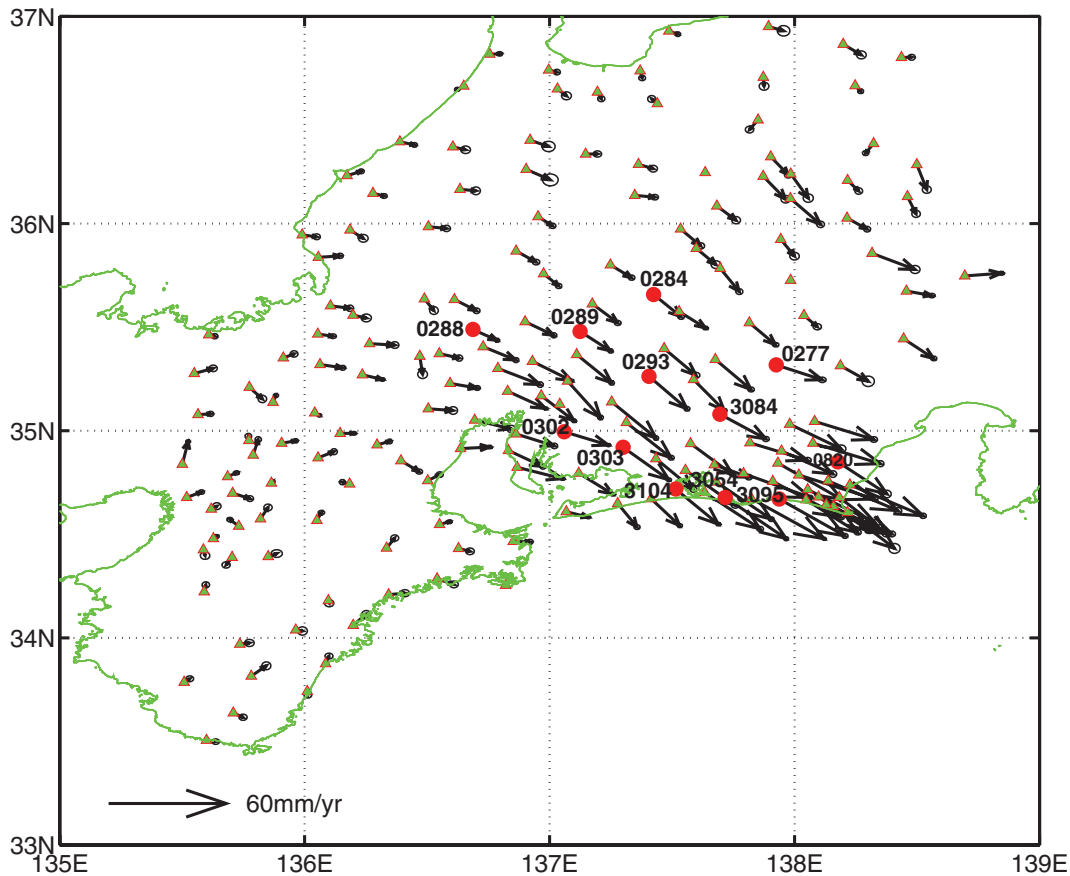


**Figure 8.** Mapview of the GPS stations and total displacements in the Tokai slow slip event. The displacement is calculated between mean position in 2002.8–2003.0 and projected position using estimated rate during 1998–2000.0. Red dots are stations whose time-series and model fit are shown in Fig. 10.

duration of days or weeks (Hirose & Obara 2006; Nakata *et al.* 2008).

## 5 DISCUSSION

### 5.1 Possible mechanisms for the spatio-temporal correlation between L-SSE and LFEs

There have been several studies that concentrated on the correlation between S-SSE (with duration of days) and non-volcanic tremor (e.g. Rogers & Dragert 2003; Obara *et al.* 2004; Hirose & Obara 2005, 2006; Ito *et al.* 2007; Schwartz & Rokosky 2007; Nakata *et al.* 2008). Only a few studies have demonstrated a possible correlation between L-SSEs, with typical durations of years, and processes with durations of hours (e.g. LFE, tremor). These studies include those of Hirose & Obara (2005) and Ozawa *et al.* (2004, 2007), focusing on Japan, and that of Peterson & Christensen (2009), which focused on Alaska. Our results show that there is a clear spatiotemporal correlation between long-term slip transients and short-term LFEs in both the Tokai and Bungo Channel region. We discuss several hypotheses that could explain such a correlation.

The first hypothesis is that both geodetic and seismic signals arise from the same physical process. This hypothesis has been proposed to explain observed temporal correspondences between S-SSEs and non-volcanic tremors or LFEs (Hirose & Obara 2005; Ide *et al.* 2008). The tremor, LFE and S-SSEs all occur in the

depth range of 30–40 km with overlapping source regions (Hirose & Obara 2005). These phenomena all seem to relate to shear slip on the plate interface (Shelly *et al.* 2006; Ide *et al.* 2007a,b), and the tremor appears to consist of sequences of LFEs (Shelly *et al.* 2007a). Although this hypothesis may be reasonable for S-SSE, tremor and LFEs, we consider it unlikely for L-SSEs. First, the majority of the slip in the L-SSEs we resolve in this study does not occur in the same region as the LFEs. In contrast our results show that the L-SSEs occur updip of the LFEs (Figs 4 and 9). Second, the total moment of LFEs in the Bungo Channel and Tokai region are on the order of  $\sim 10^{12}$ – $10^{13}$  N m, six to seven orders of magnitude less than the moment release of the L-SSEs.

The second hypothesis is that SSEs, tremor or LFEs are due to different physical processes, but occur coincidentally in time because they are triggered by a common source (Schwartz & Rokosky 2007). For example, fluid outflow due to the dehydration of the subducting slab may lubricate the fault surface and promote aseismic slip by a reduction in effective normal stress, and trigger tremor or LFEs by dissipation and promotion of microcracks in the overlying crust. Although we cannot rule out this possibility, it is not clear if such fluid bursts could be maintained over the duration of the L-SSEs in the Bungo Channel and Tokai regions. The triggering of tremors by passing surface waves of large earthquakes also suggests that other causes (e.g. dynamic triggering) may play at least a partial role (Miyazawa & Brodsky 2008; Peng *et al.* 2008).

A third hypothesis may be that the LFEs are driven by the L-SSEs. Recent studies in Kilauea, the Salton Trough, and New Zealand

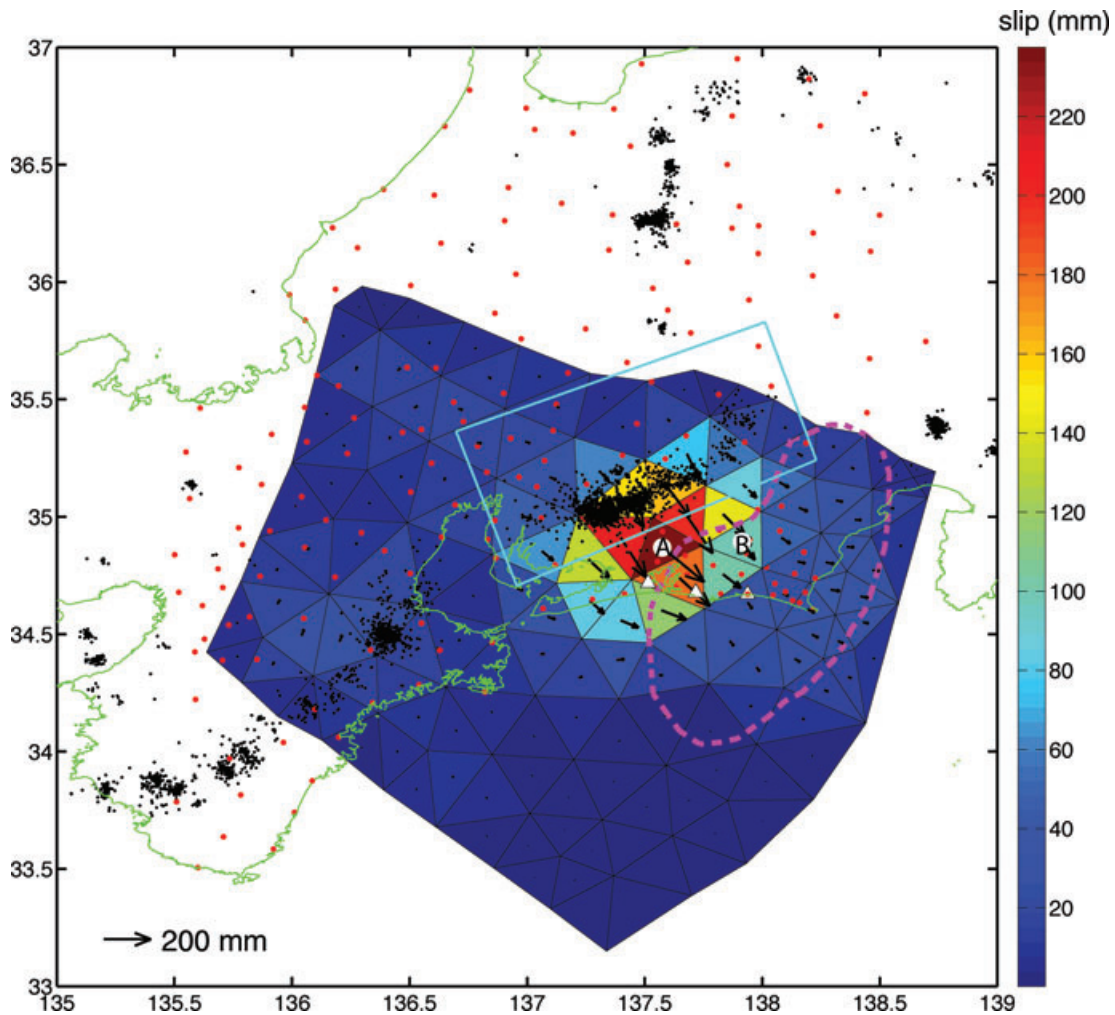


**Figure 9.** Total slip in the Tokai slow slip event during the period of 2000–2004.67. Red dots are GPS stations used in the inversion. White circle is the selected fault patch whose slip rate variation is compared to low frequency earthquake occurrence in Fig. 13. Black arrows are projected slip vectors. Black dots are epicentres of low frequency earthquakes (LFE). Only LFEs in the cyan rectangle are considered in Fig. 13. Thick dotted magenta line is the anticipated focal zone of future Tokai earthquake (Central Disaster Management Council 2001).

demonstrate that stress transfer from transient slip can trigger earthquake swarms (Segall *et al.* 2006; Lohman & McGuire 2007; Reyners & Bannister 2007; Delahaye *et al.* 2009). We investigated, but do not present, the static Coulomb failure stress change ( $\Delta\text{CFS}$ ) on the plate interface due to the transient slip in the Bungo Channel and Tokai L-SSEs, assuming that the LFEs occurred on the plate interface. We find no clear correspondence between the locations of the LFEs and regions of increased Coulomb failure stress. This may indicate that the LFEs are not caused by the transient slip in the L-SSEs; however, it may also be that the LFEs occur on cracks near the subduction interface, but do not occur on the main plate interface or on faults oriented the same as the megathrust, in which case our  $\Delta\text{CFS}$  calculations may not be applicable. Finally, the stress interactions between the L-SSE and the LFEs may be more complicated than simple static stress triggering.

## 5.2 Relation to the interplate coupling

In Figs 14 and 15, we compare the total fault slip in the Bungo Channel and Tokai L-SSEs to inferred plate coupling and the locations of LFEs in the Shikoku-Kii Peninsula and Tokai regions. Also

shown are the isothermal lines from the updated thermal model of Yoshioka & Murakami (2007). The plate coupling model is from our recent study using GPS estimates of interseismic velocities from 1996 to 2006 (Liu *et al.* 2010). We estimated plate coupling along the plate interface through a backslip inversion of both the horizontal and vertical velocity field. For the sites that are affected by the L-SSEs, the velocities are estimated from the time period that has no transient perturbation. The plate coupling model shows a good agreement with previous studies beneath the Shikoku and the Kii Peninsula (e.g. El-Fiky *et al.* 1999; Wallace *et al.* 2009) and the Tokai region (e.g. Ohta *et al.* 2004). Transient slip occurs downdip of the strongly coupled regions ('locked zones') but updip of the LFE locations. Beneath the Bungo Channel and western Shikoku, the downdip edge of the large transient slip area aligns roughly with the  $\sim 450^\circ\text{C}$  isotherm (Yoshioka & Murakami 2007). The correlation between LFEs and the  $\sim 450^\circ\text{C}$  isotherm indicates that LFEs may be related to phase transformation and fluid release (Yoshioka & Murakami 2007).

The transient slip in the 2002–2004 Bungo Channel event occurs in a partially locked zone over depths of  $\sim 20$ – $30$  km (Fig. 14). In the region of the L-SSE, the slip-deficit rate is  $\sim 50$  mm  $\text{yr}^{-1}$ , so  $\sim 300$  mm of slip-deficit accumulated over the past 6 yr since the

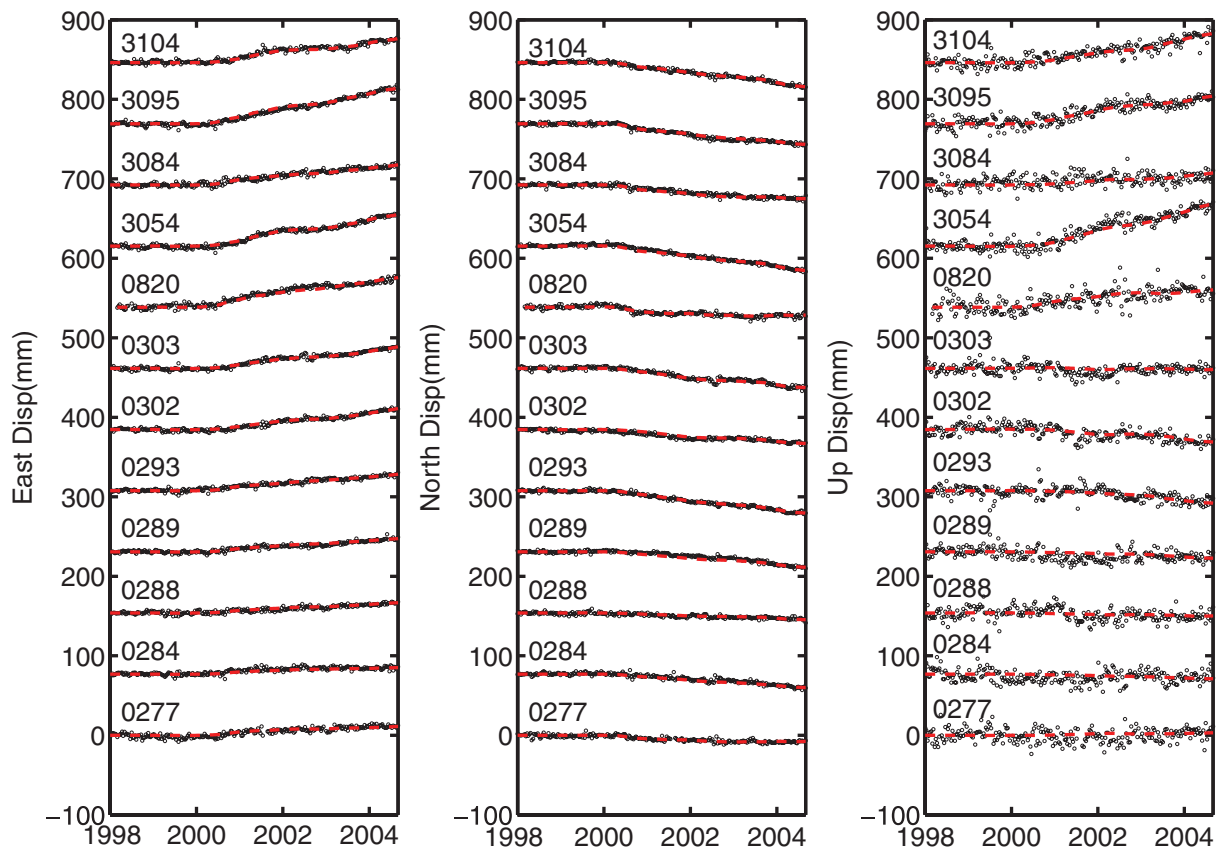


**Figure 10.** Predicted (red dashed line) and observed (black circles) position time-series at selected stations for the Tokai slow slip event. The data have been corrected for the reference frame error and a linear trend, but contain benchmark wobble noise. The model prediction is the predicted displacement from the Tokai transient slip model. The locations of the selected stations are indicated in Fig. 8.

last SSE (1996–1998). The estimated maximum slip is  $\sim 260$  mm, suggesting that episodic SSEs release a large portion of the accumulated elastic strain in this part of plate boundary. In the Bungo Channel, the overlap of transient slip and the locked region suggests that the frictional transition from velocity weakening to velocity strengthening occurs in the shallow portion of the subduction interface (Schwartz & Rokosky 2007).

In Tokai, the slow transient slip mainly occurs at the downdip edge of the strongly coupled region (Fig. 15), suggesting that the frictional properties transition from velocity weakening to velocity strengthening at the downdip edge of the locked zone. There is a small portion of the transient slip in this locked zone (Fig. 15), possibly indicating that this region of the fault surface is conditionally stable (e.g. Scholz 1998). Accounting for the transient slip, we estimate that the entire Tokai segment is recharging at a rate of  $\sim 1.9 \times 10^{19}$  N m yr $^{-1}$ . If a future earthquake ruptures the entire Tokai segment and fully releases the accumulated elastic strain since 1854, we would expect an  $M_w \sim 8.2$  earthquake assuming a shear modulus of 30 GPa. If a future earthquake ruptures only the anticipated focal zone as proposed by Center Disaster Management Council (2001), then a  $M_w \sim 7.9$  event would be expected. We also find that the region of the anticipated earthquake corresponds well to the region of maximum slip-deficit accumulation.

### 5.3 Constant low-stress drop vs. constant slip model

Ide *et al.* (2007a) proposed a unified scaling law for the relationship between moment  $M_0$  and duration  $T$  for slow earthquakes, in which

$M_0$  is proportional to  $T$ . Despite large differences in size and duration compared to other short-term processes, we find our resolved moment and duration for both the Tokai and Bungo Channel events follow this scaling law. Ide *et al.* (2007a) proposed two hypotheses to explain the relation between length scale ( $L$ ) of slip transient and duration ( $T$ ): the constant low-stress drop model, where the cube of length,  $L$ , is proportional to  $T$  ( $L^3 \propto C_1 * T$ ), and the constant slip model, where  $L^2 \propto C_2 * T$ . We test these two hypotheses using our inferred slip for both events. We infer length scales of  $\sim 150$  km for the Tokai and  $\sim 110$  km for the Bungo Channel SSE, with corresponding durations of  $\sim 4.67$  and  $\sim 2.5$  yr, respectively. We find that the event duration is more closely proportional to  $L^2$  for these two events, which suggests that a constant slip model is preferred. We further estimate average propagation velocities of  $\sim 44$  and  $\sim 45$  km yr $^{-1}$  for the Bungo Channel and Tokai SSEs, respectively. These estimates are much slower than the propagation velocities previously suggested for short-term slow earthquakes. For example, slip transients in tremor episodes migrate at  $\sim 10$  km d $^{-1}$  along-strike and  $\sim 25$ – $150$  km hr $^{-1}$  along slab dip direction in western Shikoku (Shelly *et al.* 2007b). Our slower estimates of slip propagation along strike are more consistent with the nearly stationary slip shown in Figs 6 and 11. The constant slip model implies that slip is limited by accumulated plate motion (Ide *et al.* 2007a). The relation between length squared and duration also implies the involvement of a diffusion-like physical mechanism, which could be explained by fluid movement. The hypothesis of fluid involvement is consistent with recent findings that the source regions of both long- and short-term SSE and tremor/LFE coincide with high  $V_p/V_s$  zones

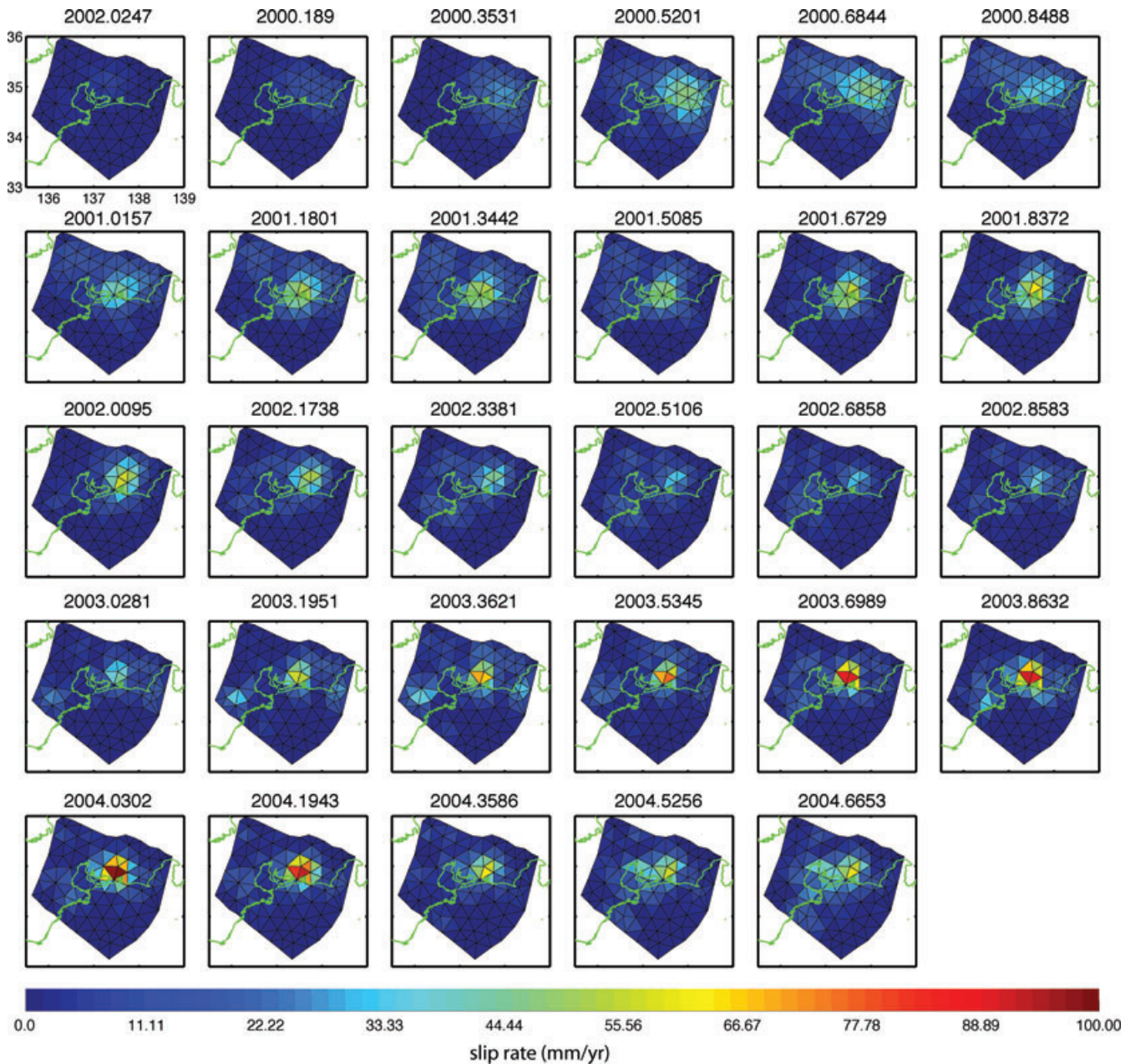


**Figure 11.** Spatio-temporal evolution of the transient slip for the Tokai slow slip event in the period of 2000–2005. Subplots represent the snapshot of slip rate at a 60 d interval. Peak slip rate is  $\sim 100 \text{ mm yr}^{-1}$ .

that can be attributed to the dehydration of subducting oceanic crust (Matsubara *et al.* 2009).

#### 5.4 Comparison with other studies

Compared to the past studies of the 2002–2004 Bungo Channel SSE, here we consider potential transient slip over a longer time period (2000–2005). Choosing a shorter modelling period risks missing early-stage slip signals and affects slip estimates. Indeed, Ozawa *et al.* (2004, 2007) used data in different periods and got different slip histories. Moreover, we image an earlier subevent that initiated in mid-2002, which was not imaged by Ozawa *et al.* (2007). Although Ozawa *et al.* (2007) does notice a small bulge-like feature

in this time, the subevent is more pronounced in our time history of the fault slip. We find that the main slip subevent initiated in early 2003, accelerated in late 2003–early 2004, and gradually subsided after early 2004. These features are in general agreement with the transient slip inferred by Ozawa *et al.* (2007). However, we find there is a clear southwestward expansion for the high slip area, in contrast to northeastward expansion suggested by Ozawa *et al.* (2007). Such differences may be due to the irregular sparse time intervals that Ozawa *et al.* (2007) used to characterize slip variation, which can have the effect of smearing out the slip details.

Our model of the 2002–2004 Bungo Channel SSE shows very similar spatiotemporal slip variations to the 1996–1998 event as imaged by Ozawa (Ozawa *et al.* 2001, 2007). This, along with other similarities as noted by Ozawa *et al.* (2004), provide strong support

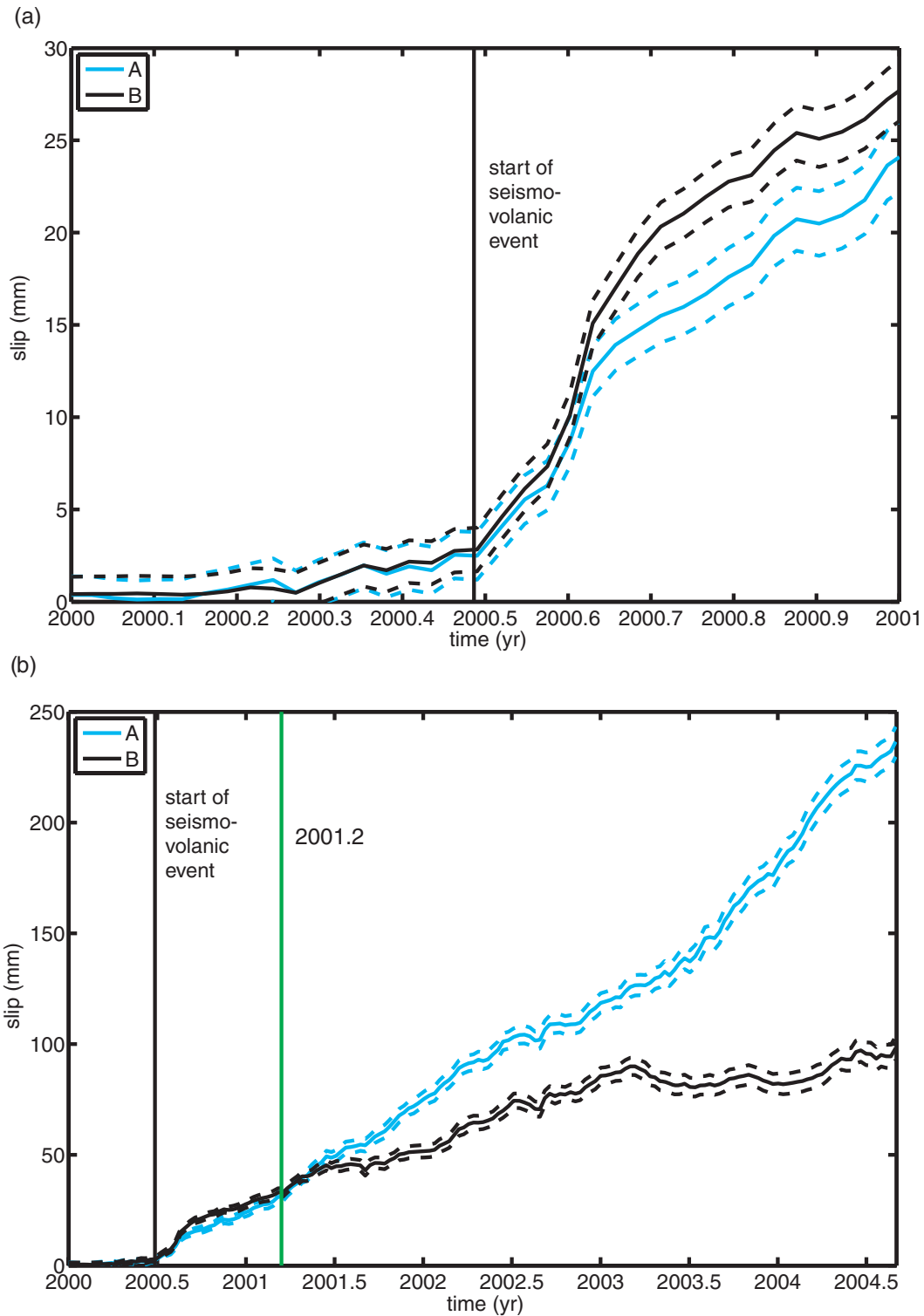


**Figure 12.** (a) The forward slip variation at the selected locations, patch A and B as indicated in Fig. 9. Dashed lines show  $1\sigma$  uncertainties. Only slip during 2000–2001 is plotted for better view. (b) Slip variation at the same locations as in (a) but over the period of 2000–2004.67. Vertical lines indicate the onset of Miyaki-Kozu seismovolcanic event (2000.4836, black) and the time when the slip at patch A starts to exceed the slip at patch B (2001.2, green).

to the hypothesis that these two events are characteristic events with recurrent intervals of  $\sim 6$  yr. Both our study and Ozawa *et al.* (2004, 2007) find LFEs locate at the downdip edge of the slow slip area. However, our analysis shows clear temporal correlation between long term slow slip event and LFEs. The equivalent  $M_w$  for the

Bungo Channel SSE is  $\sim 7.0$ , slightly smaller than the  $M_w \sim 7.1$  in Ozawa *et al.* (2007) but more consistent with his earlier estimates  $M_w \sim 7.0$  (Ozawa *et al.* 2004).

For the Tokai SSE, the transient slip in our model concentrates at the downdip transition zone centred around Lake Hamana

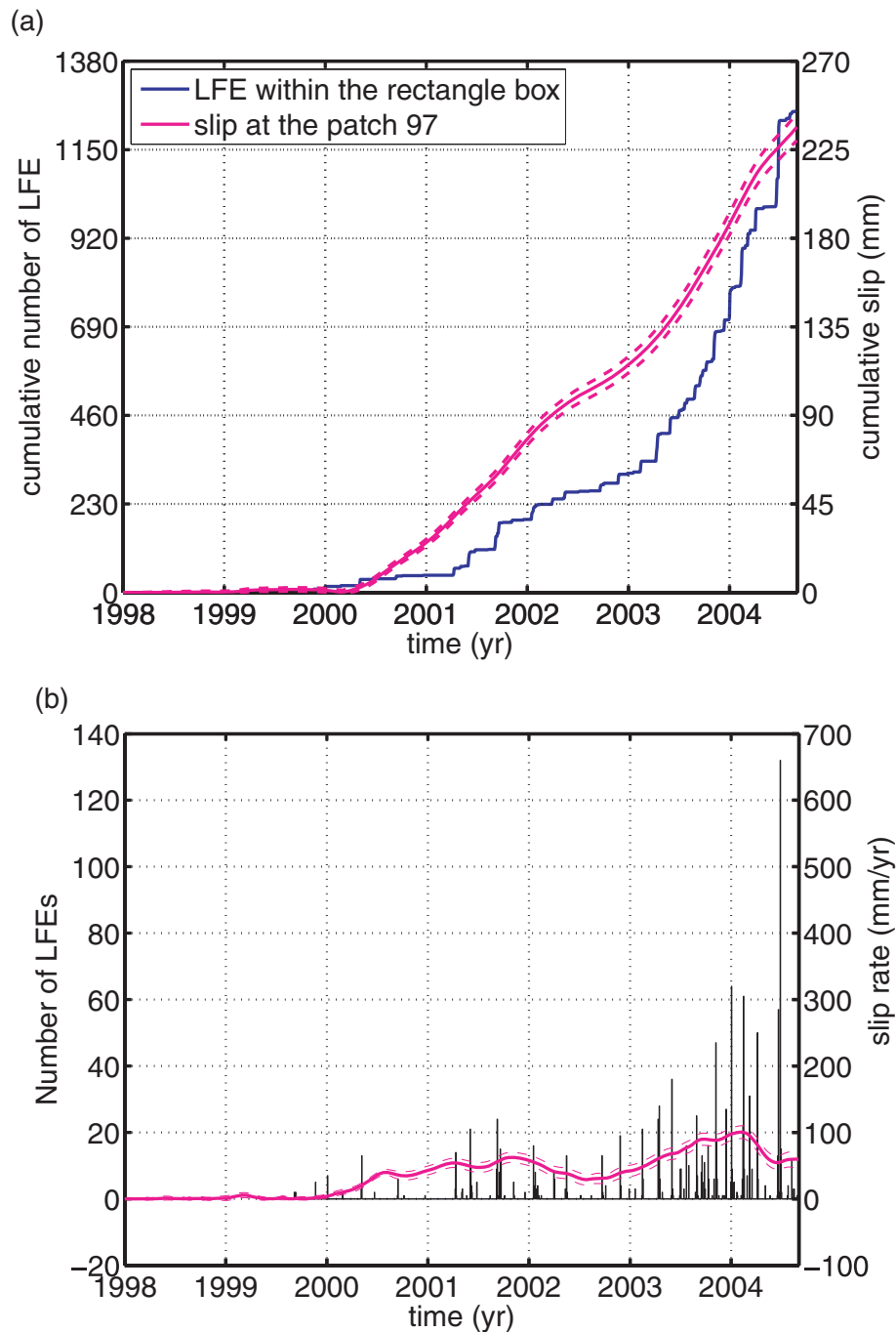


**Figure 13.** Temporal correlation between the slip (a) and slip rate (b) at the selected fault patch indicated in Fig. 9 and low frequency earthquakes within the rectangle in Fig. 9. (a) Cumulative slip compared to the cumulative number of LFEs. Magenta line represents slip. Dashed lines are  $1\sigma$  uncertainty bounds. (b) Slip rate and occurrence of LFEs. Histogram depicts the LFE occurrence, and dashed lines represent  $1\sigma$  uncertainty bounds for the slip rate.

on the western edge of the anticipated Tokai earthquake zone, consistent with previous studies (Ozawa *et al.* 2002; Ohta *et al.* 2004; Miyazaki *et al.* 2006). We observe that transient slip shifts to the northeast of Lake Hamana at about late 2001–2002, and that there is renewed slip activity to the north of Lake Hamana from 2003 to 2004. This is in general agreement with Ozawa *et al.* (2005); however, our result reveals that what Ozawa *et al.* (2005) imaged as only a relative increase in transient slip in 2003 is actually a distinct slip subevent that initiated in early 2003, reached peak slip in early 2004, and then subsided afterwards. We also infer that

the slip area that developed around Lake Hamana from  $\sim 2000.8$  to  $\sim 2001.8$  shifts to the northeast from late 2001 to 2002. The second region of transient slip qualitatively corresponds to the second slip locus as imaged by Miyazaki *et al.* (2006). We observe good temporal correlation between long-term slip transient and adjacent LFEs. Our results show that the Miyake-Kozu volcanic event postdates the start of the Tokai SSE. Our results show a coherent yet low amplitude slip initiation to the east of Lake Hamana prior to the onset of the volcanic event on 2000 June 26 (Figs 11 and 12), and that transient slip begins to propagate towards Lake Hamana



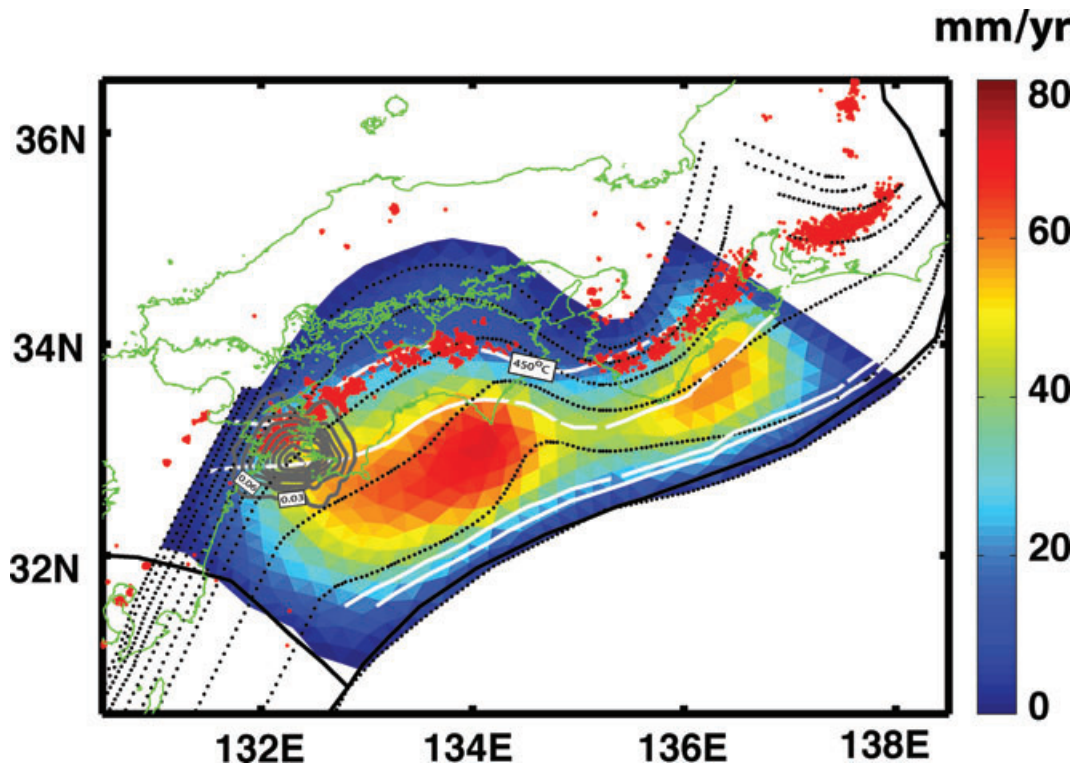


**Figure 14.** Spatial relationship between the slip-deficit accumulation rate inferred by Liu *et al.* (2010), transient slip, and low frequency earthquakes (LFE) in the Bungo Channel and Kii Peninsula. Red dots are LFEs from the Japanese Meteorological Agency. Grey lines are slip contours from the 2002–2004 Bungo Channel slow slip event. The contours are plotted at an interval of 0.03 m. The downdip extension of the coupling and low frequency earthquake are bounded by  $\sim 450$  °C isothermal temperature (Yoshioka & Murakami 2007).

around  $\sim 2000.7$ . Miyazaki *et al.* (2006) found that the slip prior to the Miyaki-Kozu volcanic event initiates slightly northwest of Lake Hamana then propagates to the southeast although their resolved slip is generally below the slip uncertainty level. It is difficult to determine what might cause such a difference, and there are considerable differences between ours and previous studies in terms of data processing, station coverage, modelling period, fault geometry, and smoothing. Nevertheless, the general features among these studies are quite consistent. Noticeably the signal strength before 2000.4846 is quite small with the total slip of  $\sim 8$  mm and expected surface displacement of  $\sim 3.5$  mm, close to the repeatability level of the cleaned time-series. It is possible that different data periods and modelling constraints adopted by individual studies may affect the detection and imaging of such small signals. Miyazaki *et al.* (2006) used 14-d average position time-series from 2000 January to 2002 December and assumed zero slip at the beginning of the modelling period. We are concerned that using too short a data period prior to 2000 June 26 may impose too strong an influence on the filter from the zero slip constraint assumed at the start of the analysis, and thus affect its capability to resolve emerging slip deformation signals.

### 5.5 Implications for physical modelling of the slow slip processes

The physical mechanism for SSE has yet to be understood. So far most numerical simulations are carried out in the framework of rate- and state-dependent friction and adopt *ad hoc* frictional parameters in order to reproduce certain features of SSE (e.g. location, recurrence interval) (Yoshida & Kato 2003; Kuroki *et al.* 2004; Liu &

Rice 2005, 2007; Shibasaki & Shimamoto 2007). There is a large gap in physical modelling of the slow slip process in bridging model predicted slip and surface deformation to actual GPS measurements or inferred slip distributions from known SSE events. In that aspect, a detailed imaging of SSE in space and time as illustrated in this paper would provide strong constraints to frictional properties on the plate interface and other influencing factors. For example, the consistent locations for the recurrent Bungo Channel SSEs and repeating subevents of the Tokai SSE implies that frictional properties on the megathrust fault vary in space, possibly controlled by temperature. There may be some lateral frictional heterogeneities, in addition to the depth-dependent frictional transitioning from velocity weakening to velocity strengthening in the downdip transition zone. The overlap of the Bungo Channel SSE with seismogenic zone suggests at least part of the frictional transition occurs within the seismogenic velocity weakening zone (Schwartz & Rokosky 2007). Furthermore, increasing evidence suggests that fluid and high pore fluid pressure associated with the dehydration of young subducting slab may play an important role in generating the tremor (Shelly *et al.* 2006) and nearby SSE (Kodaira *et al.* 2004). The remote triggering of low frequency seismic tremor by sweeping surface waves from large distant earthquakes (Miyazawa *et al.* 2008), and from earth tides in southwest Japan and Cascadia (Nakata *et al.* 2008; Rubinstein *et al.* 2008) suggests that the tremor source regions are sensitive to extremely small stress perturbations, possibly due to the increased high pore fluid pressure and low effective stress. Initial attempts have been made at combining the forward physical model with surface deformation measurements to check the viability of experimentally derived frictional data (Rice & Liu 2008). However,

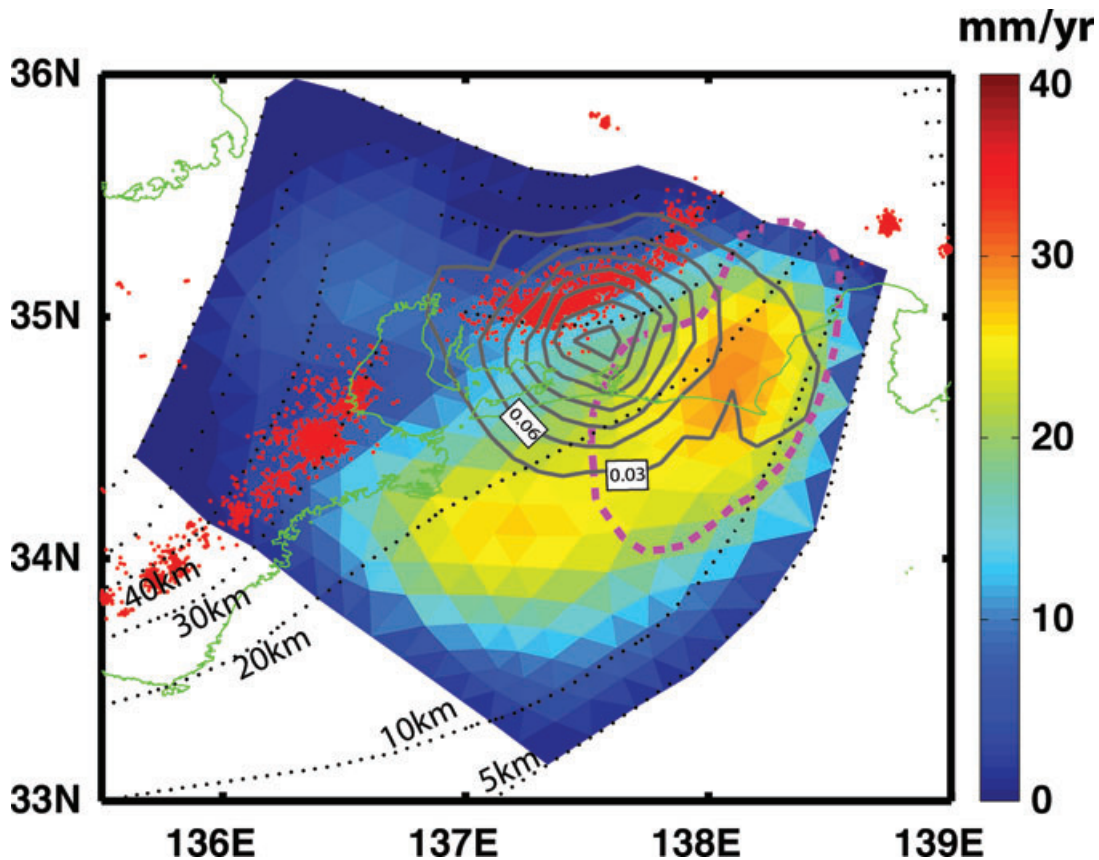


**Figure 15.** Spatial relationship between the slip-deficit accumulation rate inferred by Liu *et al.* (2010), transient slip, and low frequency earthquakes in the Tokai region. Dotted lines are iso-depth contours from Wang *et al.* (2004). Others captions refer to Fig. 14. High transient slip area generally locates at the downdip edge of strongly coupled region. Magenta curve represents anticipated source area of future Tokai earthquake proposed by Central Disaster Management Council (CDMC) (2001).

we anticipate that more realistic physical models of L-SSEs would likely involve fluid effects in addition to spatial variation in frictional properties, and should provide compatible matches to slip characteristics as revealed in this and other studies.

## 6 CONCLUSIONS

We reprocessed and analysed 10 yr of GEONET GPS data using a consistent processing and time-series analysis strategy for the entire network. We inverted these cleaned GPS time-series for the fault slip variations of two long-term transient slip events, one in the Bungo Channel and one in the Tokai region, assuming both slip events occurred on the plate interface. We find both events have complex slip histories. The Bungo Channel SSE involves two subevents. The first subevent occurred during 2002–2003 beneath the southwest part of the Bungo Channel. The second slip subevent initiated in early 2003, accelerated through 2003 and decelerated in early 2004 beneath the northeast part of the region. The high slip area of the second subevent was found to expand southwestward, different from previous estimates but more consistent with the characteristics in 1996–1998 slip event in the same region. Our analysis indicates that the Tokai slip event initiated before the Miyaki-Kozu seismovolcanic event. From late 2000 to 2001, the slip largely developed around Lake Hamana ( $\sim 137.5^\circ\text{E}$ ,  $34.7^\circ\text{N}$ ). It shifted slightly towards the northeast from late 2001, and decelerated in late 2002. There was renewed slip activity to the north of Lake Hamana in

early 2003 that reached a maximum in early 2004, and was ongoing at the end of modelling period. We observe a clear spatiotemporal correlation between the resolved slip and adjacent LFEs for both events, possibly reflecting stress modulation from long-term slip on short-term slow earthquakes. The high slip area, LFEs, and strongly coupled regions generally display a complementary spatial pattern. Direct comparison between transient slip in SSE and imaged slip deficit shows that slow slip beneath the Bungo Channel region helps to relieve at least part of the accumulated strain. Our results satisfy the unified moment-duration scaling relationship and resulting constant slip model (Ide *et al.* 2007a). The implied diffusion-like process, along with other evidence, suggests fluids due to slab dehydration may play an important role in producing slip transients and should be considered in future numerical studies on slip transients.

## ACKNOWLEDGMENTS

We thank Kelin Wang for sending us his composite plate geometry model in his paper. We also thank Akio Katsumata at Meteorological Research Institute, Japan for sending us LFE catalogue. David Shelly at USGS sent us his relocated LFE catalogue in western Shikoku. Reviews by Y. Hsu, L. Wallace, and editor J. Beavan improved this manuscript. The commercial software Gocad from Paradigm Geophysical ([www.pdgm.com](http://www.pdgm.com)) was used in fault surface modelling. The research described in this paper was carried out at

the Jet Propulsion Laboratory, California Institute of Technology, under a contract with the National Aeronautics and Space Administration and funded through the internal Research and Technology Development Program.

## REFERENCES

- Beavan, J., Wallace, L. & Fletcher, H., 2007. Slow slip events on the Hikurangi subduction interface, New Zealand, in *Dynamic Planet: Monitoring and Understanding a Dynamic Planet with Geodetic and Oceanographic Tools*, Vol. 130 of International Association of Geodesy Symposia, pp. 438–444, eds. Tregoning, P., Rizos, C., Springer, New York.
- Brooks, B.A., Foster, J.H., Bevis, M., Frazer, L.N., Wolfe, C.J. & Behn, M., 2006. Periodic slow earthquakes on the flank of Kilauea Volcano, Hawaii, *Earth planet. Sci. Lett.*, **246**(3/4), 207–216, doi:10.1016/j.epsl.2006.03.035.
- Burgmann, R., Ergintav, S., Segall, P., Hearn, E.H., McClusky, S., Reilinger, R.E., Woith, H. & Zschau, J., 2002. Time-dependent distributed afterslip on and deep below the Izmit earthquake rupture, *Bull. seism. Soc. Am.*, **92**, 126–137.
- Central Disaster Management Council, 2001. The Central Disaster Management Council of the Japanese government, Tokyo. (<http://www.bousai.go.jp/jishin/chubou/20011218/siryou2-2.pdf>)
- Cervelli, P., Segall, P., Johnson, K., Lisowski, M. & Miklius, A., 2002. Sudden aseismic fault slip on the south flank of Kilauea volcano, *Nature*, **415**, 1014–1018.
- Desbrun, M., Meyer, M., Schröder, P. & Barr, A.H., 1999. Implicit fairing of irregular meshes using diffusion and curvature flow, in *Proceedings of the 26th Annual Conference on Computer Graphics and Interactive Techniques International Conference on Computer Graphics and Interactive Techniques*, ACM Press/Addison-Wesley Publishing Co., New York, NY, 317–324, doi:10.1145/311535.311576.
- Delahaye, E.J., Townend, J., Reyners, M.E. & Rogers, G., 2009. Microseismicity but no tremor accompanying slow slip in the Hikurangi subduction zone, New Zealand, *Earth planet. Sci. Lett.*, **277**, 21–28.
- Dong, D., Herring, T.A. & King, R.W., 1998. Estimating regional deformation from a combination of space and terrestrial geodetic data, *J. Geodyn.*, **72**, 200–214.
- Dong, D., Fang, P., Bock, Y., Webb, F., Prawirodirdjo, L., Kedar, S. & Jamason, P., 2006. Spatio-temporal filtering using principal component analysis and Karhunen-Loeve expansion approaches for regional GPS network analysis, *J. geophys. Res.*, **111**, B03405, doi:10.1029/2005JB003806.
- Douglas, A., Beavan, J., Wallace, L. & Townend, J., 2005. Slow slip on the northern Hikurangi subduction interface, New Zealand, *Geophys. Res. Lett.*, **32**(16), 1–4, doi:10.1029/2005GL023607.
- Dragert, H., Wang, K. & James, T.S., 2001. A silent slip event on the deeper Cascadia subduction interface, *Science*, **292**, 1525–1528.
- Dragert, H., Wang, K. & Rogers, G., 2004. Geodetic and seismic signatures of episodic tremor and slip in the northern Cascadia subduction zone, *Earth Planets Space*, **56**, 1143–1150.
- El-Fiky, G.S., Kato, T. & Oware, E.N., 1999. Crustal deformation and interpolate coupling in the Shikoku district, Japan, as seen from continuous GPS observations, *Tectonophysics*, **314**, 387–399.
- Heki, K. & Miyazaki, S., 2001. Plate convergence and long-term crustal deformation in central Japan, *Geophys. Res. Lett.*, **28**(12), 2313–2316.
- Heki, K. & Kataoka, T., 2008. On the biannually repeating slow-slip events at the Ryukyu Trench, southwestern Japan, *J. geophys. Res.*, **113**, B11402, doi:10.1029/2008JB005739.
- Heki, K., Miyazaki, S., Takahashi, H., Kasahara, M., Kimata, F., Miura, S., Vasilenko, N.F., Ivashchenko, A. & An, K., 1999. The Amurian Plate motion and current plate kinematics in eastern Asia, *J. geophys. Res.*, **104**(B12), 29147–29155.
- Hori, T., Kato, N., Hirahara, K., Baba, T. & Kaneda, Y., 2004. A numerical simulation of earthquake cycles along the Nankai Trough in southwest Japan: lateral variation in frictional property due to the slab geometry controls the nucleation position, *Earth planet. Sci. Lett.*, **228**, 215–226.
- Hirose, H., Hirahara, K., Kimata, F., Fujii, N. & Miyazaki, S., 1999. A slow thrust slip event following the two 1996 Hyuganada earthquakes beneath the Bungo Channel, southwest Japan, *Geophys. Res. Lett.*, **26**, 3237–3240.
- Hirose, H. & Obara, K., 2006. Short-term slow slip and correlated tremor episodes in the Tokai region, central Japan, *Geophys. Res. Lett.*, **33**, L17311, doi:10.1029/2006GL026579.
- Hirose, H. & Obara, K., 2005. Repeating short- and long-term slow slip events with deep tremor activity around the Bungo Channel region, southwest Japan, *Earth Planets Space*, **57**, 961–972.
- Hsu, Y.J., Segall, P., Yu, S.B., Kuo, L. & Williams, C., 2007. Temporal and spatial variations of post-seismic deformation following the 1999 Chi-Chi, Taiwan earthquake, *Geophys. J. Int.*, **169**, 367–379, doi:10.1111/j.1365-246X.2006.03310.x
- Linde, A.T. & Sacks, S.I., 2002. Slow earthquakes and great earthquakes along the Nankai Trough, *Earth planet. Sci. Lett.*, **203**, 265–275.
- Ide, S., Beroza, G.C., Shelly, D.R. & Uchide, T., 2007a. A scaling law for slow earthquakes, *Nature*, **447**, doi:10.1038/nature05780.
- Ide, S., Shelly, D.R. & Beroza, G.C., 2007b. Mechanism of deep low frequency earthquakes: further evidence that deep non-volcanic tremor is generated by shear slip on the plate interface, *Geophys. Res. Lett.*, **34**, L03308, doi:10.1029/2006GL028890.
- Ide, S., Imanishi, K., Yoshida, Y., Beroza, G.C. & Shelly, D.R., 2008. Bridging the gap between seismically and geodetically detected slow earthquakes, *Geophys. Res. Lett.*, **35**, L10305, doi:10.1029/2008GL034014.
- Ito, Y., Obara, K., SHiomi, K., Sekine, S. & Hirose, H., 2007. Slow earthquakes coincident with episodic tremors and slow slip events, *Science*, **315**, 503–506, doi:10.1126/science.1134454.
- Jeyakumaran, M., Rudnicki, J.W. & Keer, L.M., 1992. Modeling slip zones with triangular dislocation elements, *Bull. seism. Soc. Am.*, **83**(5), 2153–2169.
- Kawamura, M. & Yamaoka, K., 2006. Spatio-temporal characteristics of the displacement field revealed with principal component analysis and the mode-rotation technique, *Tectonophysics*, **419**, 55–73, doi:10.1016/j.tecto.2006.03.019.
- Kimata, F., Hirahara, K. & Fujii, N., 2003. Repeated slow slip events and the occurrence process of the large earthquakes in the Tokai region, central Japan, in *Proceedings of the 2003 IUGG Meeting*, JSS01/30A/D-040.
- Kodaira, S., Lidaka, T., Kato, A., Park, J., Iwasaki, T. & Kaneda, Y., 2004. High pore fluid pressure may cause silent slip in the Nankai Trough, *Science*, **304**, 1295, doi:10.1126/science.1096535.
- Kostoglodov, V., Singh, S.K., Santiago, J.A., Franco, S.I., Larson, K., Lowry, A. & Bilham, R., 2003. A large silent earthquake in the Guerrero seismic gap, Mexico, *Geophys. Res. Lett.*, **30**(15), 1807, doi:10.1029/2003GL017219.
- Kuroki, H., Ito, H.M., Takayama, H. & Yoshida, A., 2004. 3-D simulation of the occurrence of slow slip events in the Tokai region with a rate- and state-dependent friction law, *Bull. seism. Soc. Am.*, **94**, 2037–2050.
- Liu, Y. & Rice, J.R., 2005. Aseismic slip transients emerge spontaneously in three-dimensional rate and state modeling of subduction earthquake sequences, *J. geophys. Res.*, **110**, B08307, doi:10.1029/2004JB003424.
- Liu, Y. & Rice, J.R., 2007. Spontaneous and triggered aseismic deformation transients in a subduction fault model, *J. geophys. Res.*, **112**, B09404, doi:10.1029/2007JB004930.
- Liu, Z. & Segall, P., 2006. Systematic search for transient deformation in southern California GPS data, *EOS, Trans. Am. geophys. Un.*, **87**(52), *Fall Meet. Suppl.*, abstract G43B-0995.
- Liu, Z., Owen, S., Dong, D., Lundgren, P., Webb, F., Hetland, E. & Simons, M., 2010. Estimation of interpolate coupling in the Nankai trough, Japan using GPS data from 1996 to 2006, *Geophys. J. Int.*, **181**, 1313–1328, doi:10.1111/j.1365-246X.2010.04600.x (this issue).
- Lowry, A., Larson, K., Kostoglodov, V. & Bilham, R., 2001. Transient slip on the subduction interface in Guerrero, southern Mexico, *Geophys. Res. Lett.*, **28**(19), 3753–3756.
- Lohman, & McGuire, 2007. Earthquake swarms driven by aseismic creep in the Salton Trough, California, *J. geophys. Res.*, **112**, B04405, doi:10.1029/2006JB004596.

- McCaffrey, R., Wallace, L. & Beavan, J., 2008. Slow slip and frictional transition at low temperature at the Hikurangi subduction zone, *Nat. Geosci.*, **1**(5), 316–320, doi:10.1038/ngeo178.
- Matsubara, M., Obara, K. & Kasahara, K., 2009. High- $V_p/V_s$  zone accompanying non-volcanic tremors and slow-slip events beneath southwestern Japan, *Tectonophysics*, **472**, 6–17, doi:10.1016/j.tecto.2008.06.013.
- Mallet, J.-L., 1989. Discrete smooth interpolation, *ACM Trans. Graph. (TOG)*, **8**(2), 121–144.
- McGuire, J. & Segall, P., 2003. Imaging of aseismic fault slip transients recorded by dense geodetic networks, *Geophys. J. Int.*, **155**, 778–788.
- Miyazaki, S., Segall, P., McGuire, J.J., Kato, T. & Hatanaka, Y., 2006. Spatial and temporal evolution of stress and slip rate during the 2000 Tokai slow earthquake, *J. geophys. Res.*, **111**, B03409, doi:10.1029/2004JB003426.
- Miyazawa, M., Brodsky, E.E. & Mori, J., 2008. Learning from dynamic triggering of low-frequency tremor in subduction zones, *Earth Planets Space*, **60**, e17–e20.
- Miyazawa, M. & Brodsky, E.E., 2008. Deep low-frequency tremor that correlates with passing surface waves, *J. geophys. Res.*, **113**, B01307, doi:10.1029/2006JB004890.
- Montgomery-Brown, E.K., Segall, P. & Miklius, A., 2009. Kilauea slow slip events: identification, source inversions, and relation to seismicity, *J. geophys. Res.*, **114**, B00A03, doi:10.1029/2005GL025087.
- Murray, J.R. & Segall, P., 2005. Spatio-temporal evolution of a transient slip event on the San Andreas fault near Parkfield, California, *J. geophys. Res.*, **110**, B09407, doi:10.1029/2005JB003651.
- Nakajima, J. & Hasegawa, A., 2007. Subduction of the Philippine Sea Plate beneath southwestern Japan: slab geometry and its relationship to arc magmatism, *J. geophys. Res.*, **112**, B08306, doi:10.1029/2006JB004770.
- Nakata, R., Suda, N. & Tsuruoka, H., 2008. Non-volcanic tremor resulting from the combined effect of earth tides and slow slip events, *Nat. Geosci.*, **1**, doi:10.1038/ngeo288.
- Obara, K., Hirose, H., Yamamizu, F. & Kasahara, K., 2004. Episodic slow slip events accompanied by non-volcanic tremors in southwest Japan subduction zone, *Geophys. Res. Lett.*, **31**, L23602, doi:10.1029/2004GL020848.
- Obara, K. & Hirose, H., 2006. Non-volcanic deep low frequency tremors accompanying slow slips in the southwest Japan subduction zone, *Tectonophysics*, **417**, 33–51.
- Ohta, Y., Kimata, F. & Sagiya, T., 2004. Reexamination of the interplate coupling in the Tokai region, central Japan, based on the GPS data in 1997–2002, *Geophys. Res. Lett.*, **31**, L24604, doi:10.1029/2004GL021404.
- Ohta, Y., Freymueller, J.T., Hreinsdóttir, S. & Suito, H., 2006. A large slow slip event and the depth of the seismogenic zone in the south central Alaska subduction zone, *Earth planet. Sci. Lett.*, **247**, 108–116.
- Ozawa, S., Murakami, M. & Tada, T., 2001. Time-dependent inversion study of the slow thrust event in the Nankai trough subduction zone, southwestern Japan, *Geophys. J. Res.*, **106**(B1), 787–802.
- Ozawa, S., Murakami, M., Kaidzu, M., Toda, T., Sagiya, T., Hatanaka, Y., Yurai, H. & Nishimura, T., 2002. Detection and monitoring of ongoing aseismic slip in the Tokai region, central Japan, *Science*, **298**, 1009–1012.
- Ozawa, S., Miyazaki, S., Hatanaka, Y., Imakiire, T., Kaidzu, M. & Murakami, M., 2003. Characteristic silent earthquakes in the eastern part of the Boso peninsula, Central Japan, *Geophys. Res. Lett.*, **30**, doi:10.1029/2002GL016665.
- Ozawa, S., Hatanaka, Y., Kaidzu, M., Murakami, M., Imakiire, T. & Ishigaki, Y., 2004. Aseismic slip and low-frequency earthquakes in the Bungo Channel, southwestern Japan, *Geophys. Res. Lett.*, **31**, L07609, doi:10.1029/2003GL019381.
- Ozawa, S., Murakami, M., Kaidzu, M. & Hatanaka, Y., 2005. Transient crustal deformation in Tokai region, central Japan, until May 2004, *Earth Planets Space*, **57**, 909–915.
- Ozawa, S., Suito, H., Imakiire, T. & Murakami, M., 2007. Spatio-temporal evolution of aseismic interplate slip between 1996 and 1998 and between 2002 and 2004, in Bungo Channel, southwest Japan, *J. geophys. Res.*, **112**, B05409, doi:10.1029/2006JB004643.
- Payero, J.S., Kostoglodov, V., Shapiro, N., Mikumo, T., Iglesias, A., Pérez-Campos, X. & Clayton, R.W., 2008. Nonvolcanic tremor observed in the Mexican subduction zone, *Geophys. Res. Lett.*, **35**, L07305, doi:10.1029/2007GL032877.
- Peng, Z., Vidale, J.E., Creager, K.C., Rubinstein, J.L., Gomberg, J. & Bodin, P., 2008. Strong tremor near Parkfield, CA, excited by the 2002 Denali Fault earthquake, *Geophys. Res. Lett.*, **35**, L23305, doi:10.1029/2008GL036080.
- Peterson, C.L. & Christensen, D.H., 2009. Possible relationship between nonvolcanic tremor and the 1998–2001 slow slip event, south central Alaska, *J. geophys. Res.*, **114**, B00A06, doi:10.1029/2008JB006096.
- Reyners, M. & Bannister, S., 2007. Earthquakes triggered by slow slip at the plate interface in the Hikurangi subduction zone, New Zealand, *Geophys. Res. Lett.*, **32**(14), doi:10.1029/2007GL030511.
- Roeloffs, E.A., 2006. Evidence for aseismic deformation rate changes prior to earthquakes, *Ann. Rev. Earth planet. Sci.*, **34**, 591–627, doi:10.1146/annurev.earth.34.031405.124947.
- Rogers, G. & Dragert, H., 2003. Episodic tremor and slip on the Cascadia subduction zone: the chatter of silent slip, *Science*, **300**, 1942–1943.
- Rice, J.R. & Liu, Y., 2008. Slow slip predictions based on Gabbro dehydration and friction data compared to GPS measurements in Northern Cascadia, *EOS, Trans. Am. Geophys. Un.*, **89**(53), Fall Meet. Suppl., Abstract U32A-07.
- Rubinstein, J.L., La Rocca, M., Vidale, J.E., Creager, K.C. & Wech, A.G., 2008. Tidal modulation of nonvolcanic tremor, *Science*, **319**, 186–189.
- Sagiya, T., 2004. Interplate coupling in the Kanto District, central Japan, and the Boso Peninsula silent earthquake in May 1996, *Pure appl. Geophys.*, **161**, 2327–2342.
- Shibazaki, B. & Shimamoto, T., 2007. Modeling of short-interval silent slip events in deeper subduction interfaces considering the frictional properties at the unstable-stable transition regime, *Geophys. J. Int.*, **171**, 191–205, doi:10.1111/j.1365-246X.2007.03434.x.
- Scholz, C.H., 1998. Earthquakes and friction laws, *Nature*, **391**, 37–42.
- Schwartz, S.Y. & Rokosky, J.M., 2007. Slow slip events and seismic tremor at circum-pacific subduction zones, *Rev. Geophys.*, **45**, RG3004, doi:10.1029/2006RG000208.
- Schwartz, S.Y., Walter, J.I., Dixon, T.H., Psencik, K.C., Protti, M., Gonzalez, V., Thorwart, M. & Rabbel, W., 2008. Slow slip and tremor detected at the northern Costa Rica seismogenic zone, *EOS, Trans. Am. Geophys. Un.*, **89**, Fall Meet. Suppl., Abstract U31B-06.
- Segall, P. & Matthews, M., 1997. Time dependent inversion of geodetic data, *J. geophys. Res.*, **102**, 22 391–22 409.
- Segall, P., Burgmann, R. & Matthews, M., 2000. Time-dependent triggered afterslip following the 1989 Loma Prieta earthquake, *J. geophys. Res.*, **105**, 5615–5634.
- Segall, P.E.K., Desmarais, Shelly, D., Miklius, A. & Cervelli, P., 2006. Earthquakes triggered by silent slip events on Kilauea volcano, *Hawaii*, **442**, doi:10.1038/nature04938.
- Seno, T., 2005. The September 5, 2004 off the Kii Peninsula earthquakes as a composition of bending and collision, *Earth Planets Space*, **57**, 327–332.
- Shelly, D.R., Beroza, G.C., Ide, S. & Nakamura, S., 2006. Low frequency earthquakes in Shikoku, Japan and their relationship to episodic tremor and slip, *Nature*, **442**, 188–191.
- Shelly, D.R., Beroza, G.C. & Ide, S., 2007a. Non-volcanic tremor and low-frequency earthquake swarms, *Nature*, **446**, 305–307, doi:10.1038/nature05666.
- Shelly, D.R., Beroza, G.C. & Ide, S., 2007b. Complex evolution of transient slip derived from precise tremor locations in western Shikoku, Japan, *Geochem. Geophys. Geosyst.*, **8**, Q10014, doi:10.1029/2007GC001640.
- Szeliga, W., Melbourne, T., Santillan, M. & Miller, M., 2008. GPS constraints on 34 slow slip events within the Cascadia subduction zone, 1997–2005, *J. geophys. Res.*, **113**, B04404, doi:10.1029/2007JB004948.
- Wallace, L.M. & Beavan, J., 2006. A large slow slip event on the central Hikurangi subduction interface beneath the Manawatu region, North Island, New Zealand, *Geophys. Res. Lett.*, **33**(11), doi:10.1029/2006GL026009.
- Wallace, L.M., Ellis, S., Miyao, K., Miura, S., Beavan, J. & Goto, J., 2009. Enigmatic, highly active left-lateral shear zone in southwest

- Japan explained by aseismic ridge collision, *Geology*, **37**, 143–146, doi:10.1130/G252221A.1.
- Wang, K.L., Wada, I. & Ishikawa, Y., 2004. Stresses in the subducting slab beneath southwest Japan and relation with plate geometry, tectonic forces, slab dehydration, and damaging earthquakes, *J. geophys. Res.*, **109**, B08304, doi:10.1026/2003JB002888.
- Wech, A.G. & Creager, K.C., 2007. Cascadia tremor polarization evidence for plate interface slip, *Geophys. Res. Lett.*, **34**, L22306, doi:10.1029/2007GL031167.
- Yoshioka, S. & Murakami, K., 2007. Temperature distribution of the upper surface of the subducted Philippine Sea plate along the Nankai Trough, southwest Japan, from a three-dimensional subduction model: relation to large interplate and low-frequency earthquakes, *Geophys. J. Int.*, **171**, 302–315, doi:10.1111/j.1365-246X.2007.03510.x.
- Yoshida, S. & Kato, N., 2003. Episodic aseismic slip in a two-degree-of-freedom block-spring model, *Geophys. Res. Lett.*, **30**, 1681, doi:10.1029/2003GL017439.